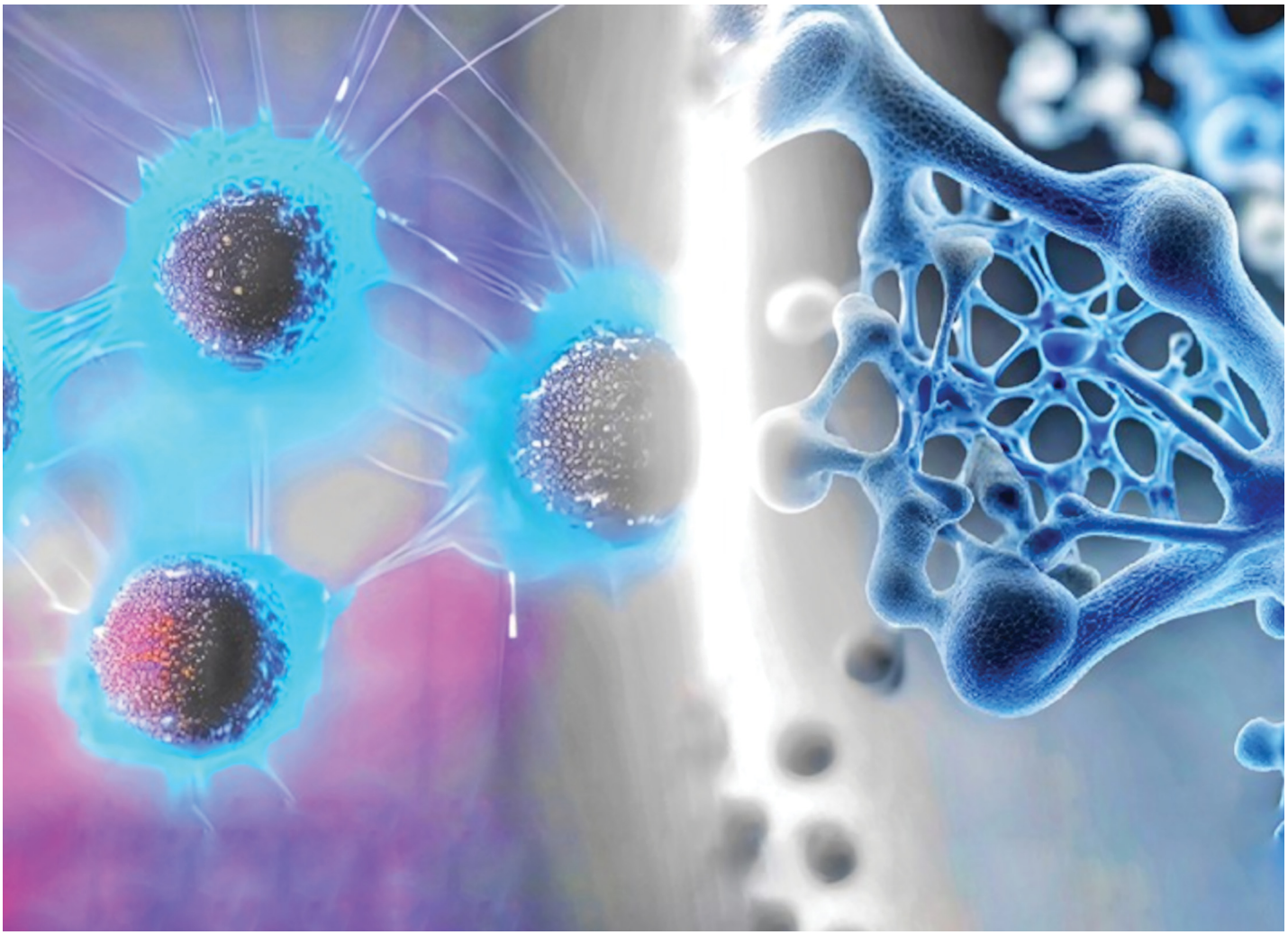

Showcasing research Professor Ana Leite Oliveira's laboratory (Biomaterials and Biomedical technology) at Centre of Biotechnology and Fine Chemistry, Faculty of Biotechnology, Catholic University, Porto, Portugal.

Tackling current production of HAp and HAp-driven biomaterials

The present work explores the latest trends in Hydroxyapatite (HAp)-based biomaterials. HAp has a well-established clinical track record, and recent efforts have focused on enhancing its properties by combining it with other materials, growth factors, and cells. 3D printing has emerged as a promising technology for these biomaterials, offering the potential for complex structures and on-demand production. However, manufacturing reproducible materials and ensuring scalability remains challenging. The limitations associated with HAp-based materials are addressed as well as the importance of continuous production for achieving uniform properties and enabling research–clinical–industry transition.

As featured in:

See João B. Costa, Ana L. Oliveira *et al.*, *Mater. Adv.*, 2023, **4**, 5453.

ROYAL SOCIETY OF CHEMISTRY

rsc.li/materials-advances

Registered charity number: 207890

Materials Advances

ROYAL SOCIETY OF CHEMISTRY

REVIEW

View Article Online
View Journal | View Issue

Cite this: *Mater. Adv.*, 2023, 4, 5453

Tackling current production of HAp and HAp-driven biomaterials

Anabela Veiga, [abc] Sara Madureira,[a] João B. Costa, [*a] Filipa Castro, [de] Fernando Rocha [bc] and Ana L. Oliveira*[a]

Received 4th July 2023,
Accepted 18th September 2023

DOI: 10.1039/d3ma00363a

rsc.li/materials-advances

Hydroxyapatite (HAp)-based biomaterials are well-established for biomedical applications due to their extensive research work and clinical track record. Recent efforts have been focusing on the development of enhanced HAp systems, through combination with other materials, growth factors, and cells. However, manufacturing reproducible materials and process scalability are still major challenges. 3D printing emerged in the last decade as a technology that allows obtaining complex structures, using HAp as a core material or by incorporating it in other organic or inorganic matrices to obtain high resolution and on-demand production. While this approach has potential, there are limitations associated with the HAp characteristics (such as particle size distribution, size, crystallinity and morphology) used during printing that need to be overcome. In this context, manufacturing high volumes of HAp with uniform properties can be achieved using continuous production, which allows for the development of highly tailored materials that can be used for 3D-printing. This review discusses the latest trends in HAp production-derived performance materials. Moreover, it fills the gap in current papers by exploring the steps required for research–clinical–industry transitions.

1. Introduction

Calcium phosphates (CaPs) are well-known bioceramics with impressive osteoconductive and osteoinductive characteristics.[1] Their bioactivity is totally dependent on the CaPs mineral phase (*e.g.*, hydroxyapatite (HAp) and tricalcium phosphate (TCP)), making them a versatile alternative for several applications since it is possible to tune different properties such as ion release, stability, solubility, and mechanical properties.[2] Synthetic HAP, in particular nano-HAp, has been widely studied in the field of biomaterials, especially for bone regeneration and replacement purposes due to its wide similarities with natural bone (*e.g.*, 1.67 calcium to phosphorus molar ratio, thermodynamic stability at pH 4.3 and above, crystallinity and size).[3] Bone implants and fillers composed of HAp show proper stabilization and fixation to the adjacent tissues, with the formation of a new, biologically active, carbonate apatite layer.[4]

However, HAp can present downsides, such as its low biodegradation rate,[5,6] and its brittle nature (unsuitable for use in weight-supporting locations).[7,8] Conventional approaches to improve the overall properties of HAp-based biomaterials consist in its conjugation with different atomic or molecular species. In this context, ion-doping has gained popularity as a chemical approach to modify the structure of HAp. This is because the crystal structure of HAp is amenable to isomorphic substitution of cations and anions with ease, leading to a wide range of potential applications in the field of biomedicine.[9] Additionally, the combination with bioactive factors (such as BMP-2, VEGF) can also enhance HAp osteoinductivity, improve stability by promoting bone growth and integration, and enable controlled release over time for the optimization of the therapeutic effect.[10–12]

In the development of HAp and HAp-hybrid biomaterials, wet synthesis methods are commonly employed as they offer a degree of control over the reaction parameters. However, these systems have some limitations associated with the lack of reproducibility.[13–15] Stirred tank reactor systems are often characterized by heterogeneous compositional distribution in the reaction medium, resulting from the lack of control of parameters such as temperature and concentration and an overall non-efficient micromixing, which affects the steadiness

[a] *CBQF-Centro de Biotecnologia e Química Fina–Laboratório Associado, Universidade Católica Portuguesa, Escola Superior de Biotecnologia, Rua Diogo Botelho 1327, 4169-005 Porto, Portugal. E-mail: aloliveira@ucp.pt, jpbcosta@ucp.pt*

[b] *LEPABE-Laboratory for Process Engineering, Environment, Biotechnology & Energy, Department of Chemical Engineering, Faculty of Engineering of the University of Porto, R. Dr Roberto Frias, 4200-465 Porto, Portugal*

[c] *ALiCE-Associate Laboratory in Chemical Engineering, Faculty of Engineering, University of Porto, Rua Dr Roberto Frias, 4200-465 Porto, Portugal*

[d] *CEB – Centre for Biological Engineering, University of Minho, Campus de Gualtar, 4710-057 Braga, Portugal*

[e] *LABBELS – Associate Laboratory in Biotechnology, Bioengineering and Microelectromechanical Systems, University of Minho, Campus de Gualtar, 4710-057 Braga, Portugal*

of the final product.[16,17] Consequently, a primary focus in current research endeavors is the establishment of new methodologies that allow reproducibility and scalability.[18] In this context, continuous production offers advantages in terms of efficiency, quality control, scalability, cost-effectiveness, and the ability to tailor product characteristics. These benefits make continuous production an attractive option for industry and researchers involved in CaP synthesis and its diverse applications.[19,20]

In the pharmaceutical industry, reactors working in continuous mode are considered cutting-edge technology for end-to-end production in a single, uninterrupted process line.[21] Continuous processes in microreactors have also been successfully applied to obtain HAp and HAp-based nanoparticle materials with controlled properties.[17,19] More recently, meso-oscillatory flow devices have been reported. In this system, the fluid is oscillated through a series of compartments or

Anabela Veiga

Anabela Veiga completed an Integrated Masters in Bioengineering in 2018 at the Faculty of Engineering of the University of Porto (FEUP) in collaboration with Abel Salazar Institute for Biomedical Science (ICBAS). She is currently doing her PhD in Biotechnology at the Faculty of Biotechnology of the Catholic University of Portugal (2021) with the theme Biofabrication of a 3D silk construct as a new strategy for Engineering a Skin Tissue Model. Before this she worked as a Project Researcher at the Laboratory for Process Engineering, Environment, Biotechnology and Energy (LEPABE), which is a research unit operating in the fields of Chemical, Environmental and Biological Engineering at FEUP in close collaboration with CBQF (Centro de Biotecnologia e Química Fina). During this time, she has worked at the Institute of Polymer Science and Technology in Madrid, Spain and in Tufts University in Medford, USA as a Fulbrighter.

Sara Madureira

Sara Madureira completed an Integrated MSc in Bioengineering – Molecular Biotechnology in 2021 in the Faculty of Engineering (FEUP) and Abel Salazar Institute for Biomedical Science (ICBAS) of the University of Porto. She also holds a BSc in Bioengineering – Biomedical Engineering, by the Faculty of Biotechnology (ESB-UCP), Portuguese Catholic University. From 2019 to 2021 she was involved in research projects at i3s (Institute for Research and Innovation in Health), where she developed her Master Thesis Magnetic Responsive Collagen-FeHap2+/3+ Coating on Porous Hydroxyapatite Scaffold for Bone Regeneration. She is currently working as a Research Fellow in CBQF (Centre for Biotechnology and Fine Chemistry) in the project Tex4Wounds-Desenvolvimento de materiais têxteis avançados para tratamento de feridas, in collaboration with Somani, Fourmag and Citeve.

João B. Costa

João Pedro Bebiano e Costa is a Scientific Researcher and Innovation Technology Manager affiliated with CBQF – Centre for Biotechnology and Fine Chemistry at UCP, Porto. Additionally, he holds the position of Professor of Tissue Engineering and Biofabrication at the Escola Superior de Biotecnologia, UCP, Porto. His research pursuits are deeply rooted in the fields of tissue engineering, biomaterials, and biofabrication, with a specific focus on 3D printing technologies for the development of personalized implants. His dedication to advancing these fields was recently recognized through a prestigious contract obtained via the Individual Call to Scientific Employment Stimulus by FCT, Portugal.

Filipa Castro

Filipa Castro is an assistant researcher at the Centre of Biological Engineering (CEB) at the University of Minho. Previously she worked as a junior researcher and Post Doc researcher in the Laboratory for Process Engineering, Environment, Biotechnology & Energy (LEPABE) of the Faculty of Engineering of the University of Porto (FEUP). She holds a Master's in Biological Engineering and a PhD in Bioengineering through the MIT-Portugal program. She has been working on both fundamentals and applications of crystallization science, in particular protein crystallization with applications to both health issues and downstream processing, and calcium phosphates precipitation. The development and characterization (hydrodynamics and mass transfer) of scaled-down multiphase reactors for both continuous and batch crystallization are also part of her research areas.

channels evenly separated by baffles. Oscillation of the fluid coupled to the baffles induces periodic changes in flow direction and intensity, creating a unique flow pattern. This oscillatory flow pattern promotes efficient mixing and enhances transport phenomena (including mass and heat transfer) by continually ensuring that reactants come into contact. Mixing intensity is governed by the oscillation amplitude and frequency.[21]

Although this approach using continuous flow reactors is gaining a lot of relevance, there are still only a few studies available to demonstrate its full potential.[17,19,21] Such a degree of control over nano-HAp production will contribute to achieving higher quality in subsequent processing steps into a bulk material or 3D construct.

In this context, three-dimensional (3D) printing has become a promising tool in tissue engineering as it allows for the creation of highly precise and customizable scaffolds to support the growth of cells into functional tissue. The processing of HAp using 3D printing allows for the creation of highly porous and intricate structures with controlled microarchitecture.[22] The ability to precisely control the composition and microstructure of HAp-composite materials opens new avenues for optimizing their biological and mechanical properties for specific medical applications.[22,23] The shift towards the implementation of large-scale 3D printing technology has been a gradual process. Nevertheless, a satisfactory solution has not yet been achieved to effectively integrate existing approaches for producing uniform and scalable HAp particles into 3D matrices. Hence, continuous productions can play a crucial preceding step in the development of customized 3D HAp constructs.

In this review, the latest developments in HAp-based biomaterials are comprehensively discussed by addressing the critical requirements and manufacturing processes involved in the light of 3D printing technology. Additionally, the significant challenges and prospective outlook of this rapidly advancing field are discussed in detail.

2. Opportunities for advanced HAp production

HAp is produced on a great scale per year to be used directly in patients or to fabricate medical devices. The batch production of this inorganic material is quite industrialized and reliable.[20]

The final properties of HAp depend on several factors such as the initial concentration of reagents used, the Ca/P molar ratio, the synthesis temperature and pH, and mixing efficiency.[11,16] In standard precipitation systems, a Ca/P of 1.67 (pure stoichiometric

Fernando Rocha

Fernando Rocha completed his PhD degree in 1984 at the Rocha University of Porto. Since then, he has worked as an Assistant Professor for the Chemical Engineering Department of the University of Porto. His research interests include crystallization of biologically relevant molecules, precipitation of calcium phosphates and composites with applications to health issues.

Ana L. Oliveira

Ana Leite Oliveira holds a PhD from the University of Minho (in 2008), collaborating with Depuy Orthopaedics, Inc. (Johnson& Johnson), USA and CSIC, Madrid, followed by a Post-Doc partnering with Tufts University, Boston, USA. She gained expertise in biomaterials for tissue regeneration, working presently in skin-related applications. She has published over 70 international peer reviewed articles and book chapters and participated in more than 100 international scientific and technological conferences, mostly as an oral presenter or as an invited lecturer. The innovation in her work generated 5 patents and links to industry, working with companies to reach new products/processes. She successfully prepared/coordinated various projects funded by National/European agencies and private companies. Presently she is the head of the Biomaterials and Biomedical Technology Laboratory at CBQF and Invited Assistant Professor at Escola Superior de Biotecnologia, Universidade Católica Portuguesa, responsible for courses in the Master of Biomedical Engineering and Bachelors' Degree in Bioengineering. Since 2008 she has been assisting the European Commission at the Research Executive Agency (REA) in the role of Expert Evaluator, Innovation Radar and Technical Monitor in several actions from FP7 and H2020 Framework Programmes.

Table 1 Common aspect ratio ranges and physicochemical alterations for HAp synthesized through precipitation

Aspect ratio range	Morphological structure	Surface area	Porosity	Mechanical properties	Cell interaction	Reported applications	Ref.
Low	Nearly spherical	Moderate	Limited	Minimal impact	Interaction with limited area	Drug delivery, scaffold fabrication	30, 31
Medium	Elongated, rod-like	Increased	Variable	Can enhance anisotropy	Enhanced attachment	Bone regeneration, drug delivery	26, 27
High	Needle-like	Increased	Increased	Potential for increased strength	Enhanced alignment	Scaffold reinforcement, bone regeneration	29

mineral HAp), physiological temperature of 37 °C, pH between 4 and 12, and low concentrations of calcium and phosphate precursor solutions promote the precipitation of the less soluble CaP (HAp) and minimize the precipitation of other calcium phosphate phases.[24,25] The resulting HAps are typically nano-sized agglomerated particles, with low crystallinity and a medium to high aspect ratio range, which refers to the ratio of its length to its width or diameter.[26–29] Spherical HAps are also reported in the literature, which have more uniform mechanical properties, lower surface areas, and subsequently lower dissolution rates[30,31] (Table 1).

The incorporation of other materials can lead to changes in these properties, which can require further optimization of the operating parameters.[24] To improve the batch-to-batch variability and fine-tuning of HAp crystallinity and nanoparticle size, continuous production can be an effective strategy for an easy scale-up.[20,32]

In terms of operation mode, continuous processes offer advantages such as the efficient use of reagents, enhanced control over operating parameters, and consistent product quality. These processes also present lower costs and footprint, while being more energy-efficient due to reduced empty-fill and heat-up cycles. Moreover, an improved yield and capacity of continuous production allow higher productivity to be achieved.[33,34] Continuous HAp precipitation methods offer the advantage of being easier to monitor and automate. However, a key challenge in implementing such methods is to achieve a perfectly mixed flow to reduce non-uniformities in the reaction medium and ensure particles suspension by minimizing concentration and temperature gradients. The attainment of a perfectly mixed flow is fundamental to the manufacturing of HAp particles with uniform attributes (*i.e.*, morphology, particle size distribution, among others).[17,35]

2.1. Continuous stirred tank reactors (CSTRs)

Plug-flow reactors (PFRs) are widely used in continuous processes and are characterized by a tubular geometry with openings on each end for reactants and products to flow through. In these systems, the contents flow like plugs, from inlet to outlet, moving along at the same speed with minimized/reduced backmixing (Fig. 1(A)).[36] The lack of axial fluid interaction is a major drawback in precipitation systems where mixing intensity plays a crucial role in the creation of a homogeneous supersaturated solution and particle suspension. Furthermore, clogging issues may occur due to the deposition and sedimentation of solids on the reactor walls, especially for long-run and high solid density experiments.[11] Thus, these reactors are more adequate for applications of gas or liquid phase systems.[36]

In continuous stirred tank reactors (CSTRs), although the reactants are also continually introduced into the reactor, and the products are concurrently collected after the reaction, the reactor contents are continuously stirred.[37–39] In similarity to mixed suspension mixed product removal (MSMPR) systems, CSTRs are equipped with stirring impellers and turbines, along with an integrated temperature control system (Fig. 1(B)).[40]

CSTRs offer a stable supersaturation due to their steady-state operation.[37] These reactors often have a high working volume and can be connected in series to conduct multiple-step processes CSTRs in cascade.[38,39] In recent years, double CSTRs set-ups to precipitate HAp have been implemented.[41] However, the deposition of reaction products, which occurs after some time of operation, is also frequent, leading to the recurrent need to stop the process and wash the reactor.[41] In addition, CSTRs are characterized by slow heat and mass transfer, *i.e.*, heterogeneous distributions of parameters such as temperature and concentration, leading to the heterogeneous distribution of supersaturation in the reaction medium. Despite achieving macromixing through stirring in CSTR and MSMPR systems, micromixing at the molecular level is not effectively controlled. While this issue is more pronounced in batch systems, it still exists in continuous setups, thereby negatively impacting the reproducibility of the process and the quality of the resulting product.[42]

The aforementioned issues are further exacerbated during scale up, described as "how to design a pilot or industrial reactor able to replicate through a standard methodology the results obtained in the laboratory".[43] CSTR mixing is intrinsically dependent on scale and laboratory scale experiments cannot reliably predict the behavior of large-scale plants, where stagnant zones and excessive shear rates at the impeller tip can limit the effectiveness of the reactor.[43] Due to these limitations, several reactors have been developed to better control the reaction conditions, thereby optimizing the final product's characteristics.[44]

2.2. Microreactors

Microreactors are scaled-down systems (dimensions in the sub-millimeter range) that have been used to produce HAp, overcoming some of the reported drawbacks of the CSTR systems. Transfer processes, as well as residence time, occur faster in these reactors, owing to their high surface-area-to-volume ratio,

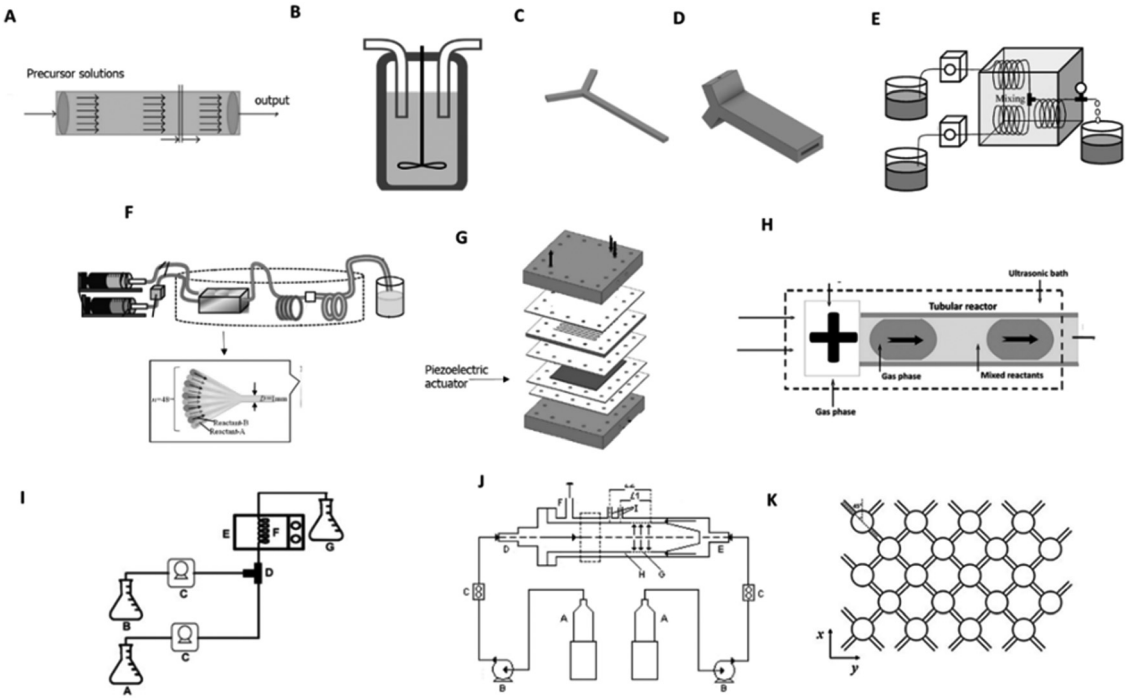

Fig. 1 Reactors applied for the continuous production of HAp: (A) plug-flow reactor; (B); conventional CSTRs;[38,39] (C) tubular Y-shaped reactor;[47] (D) scaled tubular Y-shaped reactor;[48] (E) tubular T-connection reactor;[49] (F) microreactor with 48 mixing channels;[50] (G) tubular reactor with ultrasonic system;[28] (H) segmented gas–liquid flow tubular reactor;[28] (I) CSTRs system with microwave aiding apparatus;[53,54] (J) MTMCR[56] and (K) NETmix reactor.[58,59]

making these reactors interesting tools for high-throughput processing.[45] The reduced energy and reagent requirements make these devices ideal for research and development activities. Moreover, process optimization and scalability are also considerably easier, either by increasing the running time or by running reactions in parallel (a process known as scale-out).[13,46] For these reasons, several microreactor configurations have been developed and applied in HAp-manufacturing procedures.

2.2.1. Tubular reactors. Various types of tubular reactors have been documented, with the prevalent configuration featuring two input channels and one reaction channel that come together at a T-junction or Y-shaped junction. At this juncture, the reactants collide before progressing through the reaction channel as the chemical reaction takes place.[47–49]

Y-shaped reactors using 3D printing technology have been recently reported to obtain structures with precise geometry and channel dimensions. In the reported works a fused deposition modeling (FDM) technique was implemented using acrylonitrile butadiene styrene (ABS) polymer, which is stable under the conditions of the HAp precipitation and provides the necessary durability for the pressure used in the reaction system.[47,48]

Latocha *et al.*[47] used two Y-shaped continuous reactors of different lengths, operating at atmospheric pressure and room temperature to produce nano-HAp and spherical, lecithin-modified nano-HAp (Fig. 1(C)). Although the methodology used was successful, the small dimensions of the reactor resulted in a low production rate. In the work of Wojasiński *et al.*,[48] this problem was minimized by scaling up and numbering up this reactor (Fig. 1(D)).

Some alternative setups have been proposed to guarantee the mixing of the precursor solutions. Fujii and co-authors proposed a continuous flow tube reactor in which two plunger pumps are connected to a T-shaped mixing unit and a polytetrafluoroethylene (PTFE) reaction tube. In this system, the mixing of the precursor solutions is achieved before and after precipitation by using a coiled structure (Fig. 1(E)).[49] This approach is considered a passive mixing mechanism since it focuses on changing the reactor geometry to improve its mixture. Nano-HAps were also effectively obtained by adding a microreactor unit with 48 channels before a coiled structure, each with a width of 1 mm to enable uniform mixing of suspensions on the micrometer order (Fig. 1(F)).[50]

A different approach followed by Castro *et al.*,[28] to assure appropriate mixing and minimize HAp aggregation, was the implementation of an integrated piezoelectric element in a microreactor to allow direct transmission of ultrasound (Fig. 1(G)). The reported reactor led to a significant reduction in particle aggregation.[28] Lorenzo *et al.*,[51] achieved a similar effect by immersing a tubular reactor in a bath with a sonicator.

Segmented flow reactors are also an alternative for HAp production and can narrow residence time distribution (Fig. 1(H)). In these reactors, reactants are segregated by immiscible fluids to form bubbles (gas in liquid) or droplets (dispersed liquid in a carrier liquid).[52] Microwave heating has also been used for

continuous HAp production, as an optional energy source (the application of high frequency electric fields induces heating through the dipolar polarization of polarized molecules resulting from chemical bonds) (Fig. 1(I)).[53,54]

Although the continuous processes implemented have been successful in the synthesis of HAp, the need for special types of equipment and complex set-ups can restrict its use to a laboratory scale.[21]

2.2.2. Industrial scale microreactors. Scaling up of microreactors is the focus of many researchers that aim to increase the throughput while preserving the reaction physics and channel flow hydrodynamics to obtain particles with more uniform characteristics at higher quantities, more suitable for industrial processes. One of the most important issues when stepping out of laboratory-scale is how to ensure flow equidistribution with minimal pressure loss in each microchannel.[55]

Yang *et al.*,[56] adopted a microporous tube-in-tube microchannel reactor (MTMCR), which consists of two coaxial tubes, *i.e.*, the outer tube and the inner tube, forming an annular microchannel. The liquid in the inner tube through the annular micropore belt is dispersed into several small streams, followed by the high-speed impinging with the laminar flow in the chamber between inner and outer tubes. The structure of the annular microchannel greatly enlarges the throughput of MTMCR, compared to other microreactors (Fig. 1(J)).

The NETmix Reactor is another example of modified microreactors that is currently used in FLUIDINOVA, a company that focuses on the production of HAp-driven materials for medical, oral, and food applications.[57] This device consists of a network of several mixing chambers interconnected by channels oriented at a 45° angle from the main flow direction. Reactants are injected at the inlet channels. Mixing occurs in these chambers when the two streams coming from each channel meet (Fig. 1(K)).[58,59]

Nevertheless, the reported reactors are associated with some disadvantages. Microreactors are usually characterized by geometries with a low Reynolds number (Re), which is the ratio of inertial forces to viscous forces. When Re is large, inertial forces dominate over the viscous forces, the fluid is flowing faster and the flow is turbulent. On the other hand, when Re is low, the viscous forces are dominant, and disturbances in the flow are damped out by viscosity. In this case, fluid particles are kept in line generating a laminar flow. In microreactor channels, laminar flow is dominant and is characterized by a parabolic velocity profile, leading to residence time distributions. The parabolic velocity profile and obstruction, by wall attachment of particles and by particle aggregation, limits the use of these reactors.[16] This hinders the handling of solid particles and the overall transportation efficiency of the process.

2.3. Oscillatory flow reactors (OFRs)

2.3.1. Conventional OFRs. Oscillatory flow reactors (OFRs) have been proposed in the literature as an alternative to stirred tank and tubular reactors due to their superior mixing and efficient heat and mass transfer capabilities, particularly in liquid–liquid systems or for homogeneously suspending solid particles.[19,32,34]

OFRs are operated under oscillatory flow mixing (OFM), which occurs when the reactor is comprised of uniformly spaced orifice deflectors called baffles, and a liquid or a multiphase mixture is oscillated in the axial direction by means of diaphragms, bellows or pistons. The generated flow accelerates and decelerates according to a sinusoidal velocity–time function. The interaction of the flow with the baffles generates vortex rings, which are formed downstream of the baffles. When the flow decelerates these vortices move into the centre of the reactor, where a well-mixed and uniform region is generated.[60,61]

The intensity of mixing can be varied by tuning the oscillatory conditions (amplitude (x_0) and frequency (f) of oscillation) and several different mixing regimes have been identified, ranging from laminar to fully turbulent flow. The ability to generate radial mixing gives a unique form of control with respect to the intensity of mixing, axial dispersion and transfer processes.[62,63]

Mixing is influenced by a combination of different geometric parameters and operational parameters (baffle area, baffle spacing, baffle thickness, oscillation frequency, and amplitude). The major advantage over tubular reactors, where mixing is dependent on the applied flow rate, is that in OFR mixing is essentially controlled by the oscillation frequency and amplitude. Hence, since mixing is independent of flow rate, it implies that OFRs can be used in processes with longer kinetics without the need to use larger tubes. In the case of tubular reactors, to increase the residence time, the flow rate must be decreased, which compromises mixing, or a tube length increase is required.[64]

2.3.2. OFR with smooth periodic constrictions (SPCs). Despite their advantages, conventional OFRs present limitations associated with the existence of dead zones or stagnate regions near the angle between the baffles and the reactor. To overcome this problem Reis *et al.*,[65] proposed an OFR with smooth periodic constrictions (SPCs) suitable for biotechnological processes at the mesoscale, reducing dead volume areas and shear stress that can be detrimental to bacterial and other cell cultures.[65]

Regarding HAp synthesis, OFRs with SPCs allows process intensification with nano-HAp particles being obtained 4 times faster than in stirred tank batch reactors, and with no intermediate CaP phases being formed.[19] In the work of Castro *et al.*,[32] HAp with controlled properties was obtained in the scaled-up OFR operating in continuous mode, demonstrating the feasibility of this technology and its innovative potential. The particle obtained also promoted cell proliferation of osteoblastic-like (Saos-2) cells[32] (Fig. 2(A)).

However, secondary nucleation, agglomeration, clogging, and solid deposition can occur.[34,61,65] To overcome the previously stated issues, and prevent solids deposition, a new design (modular oscillatory flow plate reactor) (US20190111402A1) was developed and the common circular cross-section was replaced with a rectangular one which is less prone to particle

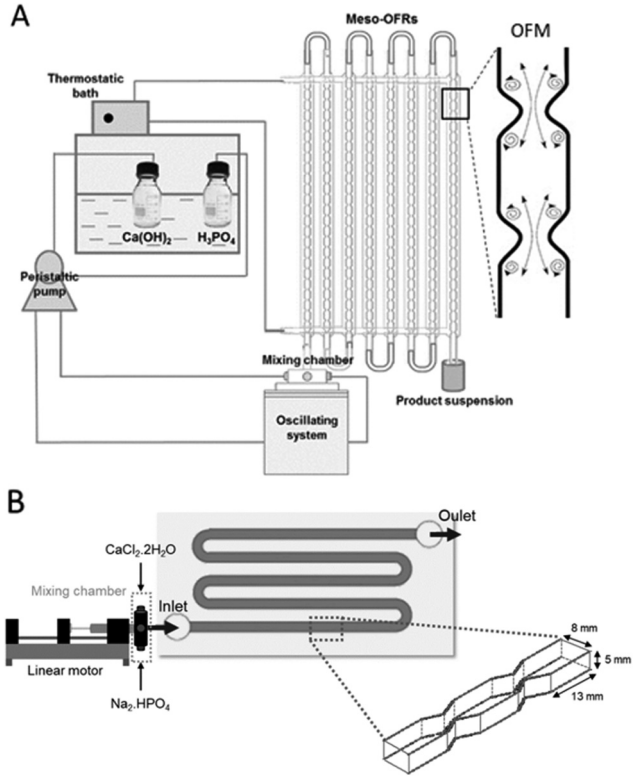

Fig. 2 (A) Scaled-up meso-OFRs and oscillatory flow mixing inside a reactor and (B) MOFPR used for continuous manufacturing of HAp particles.[14,17]

accumulation close to the constrictions compared with the circular cross-section of conventional oscillatory flow reactors with sharp baffles.[66] According to Cruz and the research team,[64] contrary to the circular cross-section, which has an undulating base where the particles can be trapped while flowing along the tube, the rectangular cross-section has a flat base where the particles can flow in a less constricted path.

2.3.3. Modular oscillatory flow plate reactor (MOFPR). The optimized reactor, that fulfils the gaps of the described OFRs is the modular oscillator flow plate reactor (MOFPR).[66] Its 2D-SPCs and rectangular cross-section with optimized geometry and dimensions enable reduced shear stress and improved solid suspension and transportation.[66] The plate reactor can be assembled and disassembled easily for cleaning, which is bound to be necessary at some point in reactors where precipitation is carried out. Furthermore, the MOFPR technology is suitable for multiphase systems applications such as HAp manufacturing.[34,67–69]

This system has been used to produce CaP particles with tailored properties for tissue engineering applications (in terms of morphology, particle size distribution and crystallinity) simply by changing the oscillation parameters (f, x_0). Moreover, other parameters such as the initial reagents concentration, initial Ca/P molar ratio, and temperature can also be easily modified in the applied process, leading to the synthesis of specific phases of CaPs in high amounts.[14] The MOFPR has also been applied in the development of hybrid HAp-particles such as HAp-sericin and HAp-sericin-cerium materials, that improve cell viability of human dermal fibroblasts.[70] Hence, MOFPRs showed promising results for the continuous production of HAp and HAp composite powders with high potential for both bone and skin-tissue engineering (Fig. 2(B)).[70,71]

This technology offers the potential to customize the production of HAp and HAp-hybrid systems, ensuring a reproductive system that serves both academic and industrial purposes. This includes synthesizing significant quantities of uniform particles essential for characterization techniques and *in vitro* viability assessments in academia, as well as ensuring batch consistency for industrial applications.

3. Advanced HAp and HAp-hybrid systems

While HAp has been widely used in tissue engineering, certain limitations, such as low mechanical strength, poor resorption properties, processing challenges, and limited bioactivity[4] have driven researchers to explore innovative approaches, such as ion doping and incorporation of bioactive factors. Ion doping aims to enhance HAp's properties by introducing various ions into its crystalline structure. This approach, driven by the ion exchangeability of HAp, brings forth new characteristics such as osteogenic activity and conferring antimicrobial properties and magnetic properties.[72–74] On the other hand, a combination of biological cues introduces the addition of growth factors and cells into the HAp framework. This strategy aims to create synergistic effects that enhance HAp's potential in tissue engineering such as promoting bone tissue formation and angiogenesis.[10]

3.1. Ion-doping

3.1.1. Enhanced osteogenic and antimicrobial activity HAp. The literature describes two HAp crystal forms: a monoclinic form in the $P2_1/b$ space group and a hexagonal form in the $P6_3/m$ space group.[4] The hexagonal phase is more common due to the susceptibility of the monoclinic form to destabilization by impurities. The hexagonal structure has two Ca sites: Ca1 (aligned with OH^- channels) and Ca2 (arranged in a staggered triangular pattern). These sites are within a phosphate assembly with parallel OH^- ion-filled channels along the crystallographic c-axis.[75] The introduction of foreign ions into the crystal lattice of HAp during its synthesis involved the following steps: (1) preparation of precursor solutions containing the ions that will be incorporated into the HAp lattice.[76,77] These precursor solutions can include calcium and phosphate sources along with the doping ions. During the precipitation process, ions from the precursor solutions are incorporated into the growing HAp crystal lattice. This can occur through two main mechanisms: (2) ion exchange or ion substitution in which OH^-, Ca^{2+}, and PO_4^{3-} can be replaced by different ions (Fig. 3). (3) As the precipitation reaction progresses, the introduced ions become integrated into the crystal lattice of HAp. (4) The doping ions occupy lattice sites that would have been

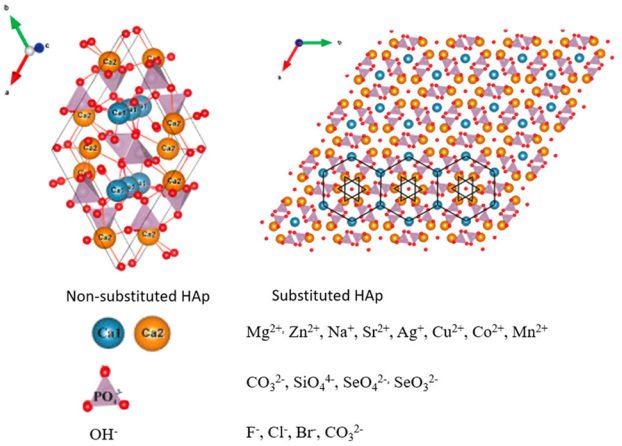

Fig. 3 Ion substitution (Ca^{2+}, PO_4^{3-} and OH^-) in the HAp lattice. Adapted from ref. 75 and 78.

occupied by the host ions if undoped HAp were forming. (5) The crystal growth of doped HAp continues as more ions are added to the lattice.[78] After substitution, HAp retains its hexagonal structure.[75–78]

These substitutions result in unique characteristics of the final molecule and are possible due to the high ion exchangeability of HAp.[79] For the bulk material, these differences can be perceived in the macro crystal morphology, mechanical properties and even biological behavior (Table 2).[4]

When considering doped HAp for biomedical purposes, two major applications can be encountered: one relating to bone healing, in the way that many substitutions enhance HAp's osteogenic activity, promoting cell proliferation and differentiation into an osteoblastic phenotype;[72,73] and other topics relate to substitutions that give rise to antimicrobial HAp.[91,92] Many times, the ions chosen for calcium substitution led to both these characteristics (enhancement of biological response and antimicrobial properties).[72,93,94]

The ions that exhibit enhanced osteogenic activity are widely acknowledged in the literature, among which strontium (Sr^{2+}) and zinc (Zn^{2+}) are the most frequently mentioned, and often combined.[93–95] Strontium alone is said to improve the mechanical properties of HAp scaffolds, and its release into cell medium can activate transduction pathways that lead to osteogenesis.[96,97] Jiang *et al.*,[96] doped HAp with Sr^{2+} ions in different percentages, from 2.5 to 20 wt%, which promoted osteogenic activity *in vitro* and led to both bone and vasculature regeneration *in vivo* and, in both scenarios, the best results were achieved with 10% Sr^{2+}.[96]

Zn^{2+} is the best example of a multipurpose ion since it is reported as an inducer of matrix mineralization towards new bone formation while presenting antimicrobial and anti-inflammatory properties.[4,91] Zn^{2+} presents osteogenic properties associated with its participation in many regulatory pathways, being a co-factor of many enzymes, and inhibiting osteoclastic activity, hence, bone resorption.[91]

Other ions that are applied in HAp substitutions that lead to enhanced bone regeneration are silicon,[98] magnesium,[4] lithium[99] and selenium[100] (Si^{2+}, Mg^{2+}, Li^+ and Se^{2-}, respectively).

Leu Alexa *et al.*,[4] doped HAp with Mg^{2+} and Zn^{2+}, separately, and developed 3D-printed scaffolds with each of the doped powders, dispersed in a polymeric matrix. They found that Mg^{2+} induced a better behavior at 5%, while Zn^{2+} did at 0.5%. Ultimately, both improved cell viability and osteogenic behavior when compared to the control (with non-doped HAp). Nonetheless, the scaffold containing Mg^{2+}-doped HAp exceeded the effects of the one containing Zn^{2+}.[4,94]

Concerning antimicrobial activity, ions such as fluoride,[72] silver,[92,101,102] zinc,[91,103] magnesium and copper (F^-, Ag^+, Zn^{2+}, Mg^{2+}, Cu^{2+}, respectively) were revealed to be a valid alternative when combined with HAp.

Although Zn^{2+} has presented osteogenic abilities, the local delivery of this ion can also act as a substitute for conventional antibiotics (it can destabilize cell membranes and deactivate enzymes[91]), which is always an advantage since bacterial resistance is a rising worldwide issue. The drawback of Zn^{2+}, as with other antimicrobial ions, is its cellular toxicity. Consequently, the integration of Zn^{2+} ions into HAp molecules represents a valuable strategy, as it enables controlled delivery and promotes appropriate bioavailability, thereby mitigating any potential toxic effects.[103]

Despite the numerous advantages of single ion substitutions, recent advancements have shifted towards the implementation of co-substitutions, where two ions are incorporated into the crystalline structure of HAp.[4,93,95,98,104,105] Another approach involves the fusion of two single substituted HAp into a single three-dimensional material. Silver is widely used as an antibacterial/antifungal substance and is present in many

Table 2 Changes that occurred with ion doping in HAp-precipitation systems

Properties	Changes that occurred with ion doping	Ions	Ref.
Mechanical strength	Ion substitution can increase compressive strength, fracture toughness, and hardness.	Sr^{2+}, Fe^{3+}	80–82
Biocompatibility	Dopants can enhance cell attachment and proliferation.	Sr^{2+}, Zn^{2+}, Li^+, Se^{4+}	83–85
Crystallinity and crystal structure	Substituting ions with different sizes and charges can affect crystallinity and lattice stability.	Zn^{2+}, Ba^{2+}, F^-, Fe^{3+}	77,82,86
Surface properties	Ion doping can alter surface charge and wettability, affecting interactions with biological tissues and fluids.	Sr^{2+}, Zn^{2+}	87,88
Optical properties	Certain dopants can introduce coloration or luminescence, which is potentially useful in imaging and diagnostics.	Fe^{2+}, Fe^{3+}, Gd^{3+}, Eu^{3+}, Co^{2+}	89
Thermal stability	Dopants can influence the material's response to temperature changes, affecting its thermal stability.	Al^{3+}	90

commercially available products, such as wound dressings. Their antibacterial effect is related to its electrostatic interaction with cell membranes resulting in its rupture.[92] Ag^+ is also highly referred to in the literature of doped HAp.[92,101,102] Sinulingga *et al.*,[106] made two variations of 2.5% Ag^+-doped HAp, one with Zn^{2+} (2.5%) and another with Mg^{2+} (2.5%),[92] in order to try to mitigate the cytotoxic effect found with previously reported 5% Ag^+-doped HAp.[106] The presence of Zn^{2+} and magnesium enhanced the antimicrobial activity (when compared to the sample with 2.5% Ag^+), since both 2.5 Ag^+/2.5 Mg^{2+} and 2.5 Ag^+/2.5 Zn^{2+} killed 99 ± 1% *E. coli* (similarly to the 5% Ag^+HAp), while presenting lower cytotoxicity towards the tested pre-osteoblastic cells.

3.1.2. Magnetic HAp. The number of routes for producing magnetic nanoparticles in the biomedical field has increased steadily over the years due to their paramagnetic and superparamagnetic behavior. In the first case particles are magnetized by an external magnetic field, aligning parallel to it in a permanent manner, while in the second, particles behave similarly to in the paramagnetic case but their magnetization ceases alongside the magnetic field.[107]

Magnetic micro and nanosystems have garnered significant attention from the scientific community due to their potential applications in various fields, including bioimaging, hyperthermia treatments, tissue regeneration, and controlled drug release.

The integration of magnetic nanoparticles into drug delivery systems has been shown to offer several advantages over conventional delivery methods. One key advantage is the ability to precisely guide the particles to the target site through the application of external magnetic fields. This ensures that the carried drug is distributed specifically to the intended region, reducing the likelihood of side effects associated with the drug, particularly in cases where the drug is toxic (such as chemotherapy drugs). In addition to targeted delivery, the release pattern of the drug is another important factor to consider. The sudden release of a high dose of the drug can lead to toxic effects, which can be mitigated by controlling the rate and pattern of drug release. Magnetic drug delivery systems have the potential to overcome this issue, as external magnetic fields can be used to modulate the release of the drug from the magnetic nanoparticles.[74] This enables the release pattern to be fine-tuned, ensuring that the drug is delivered at the optimal rate to minimize toxicity and maximize therapeutic efficacy.

Iron (Fe) doped HAp has been widely studied as a less toxic substitute for magnetite SPIONS which are, to this day, the most used magnetic nanoparticles for biomedical applications.[107–110] The cationic substitution of calcium with iron (Fe^{2+} or Fe^{3+}) induces deformations in the HAp lattice, and alters the magnetic properties of the material, from diamagnetic (pure HAp), to superparamagnetic (iron doped HAp).[79] Also, Fe-HAp can have different grain sizes, enhanced thermal stability and mechanical properties and higher bioactivity.

3.2. Combination of biological cues

3.2.1. Bioactive factors. Regarding the development of advanced HAp-based systems, the incorporation of bioactive factors is a commonly employed approach. Due to the short half-life and rapid diffusion of growth factors by body fluids, combining them with CaP can lead to the creation of controlled release systems. This is particularly important for medium to large-sized bone defects that require long-term active bone healing processes. Of the various members of the bone morphogenetic proteins (BMP) family, BMP-2 has been shown to play a crucial role in promoting osteogenesis and chondrogenesis in several clinical trials. Currently, this protein is applied in non-union bone fractures, spinal fusions, and periodontal bone regeneration.[10]

The simplest approaches to produce these biomaterials include the deposition of BMP-2 onto CaP-based scaffolds (Fig. 4(A)). Under physiological conditions of temperature (37 °C) and pH (6–8), the solubility of CaPs and, consequently, their degradation *in vivo* is higher for β-TCP than for HAp.[11,12]

According to the literature, the degradation rate of HAp can range from several months to years[11,116] depending on factors such as the size of the implant and the presence of any impurities or dopants. On the other hand, the degradation rate of β-TCP can range from several weeks to several months, with the material gradually dissolving and being replaced by new bone tissue.[117,118] As a result of the greater degradation rate, β-TCP is usually selected to develop 3D scaffolds that can effectively control BMP-2 release.[12,112,113,119,120] Moreover, the incorporation of BMP-2 leads to the formation of new bone with denser connective tissue and well-supplied with cellular components (Fig. 4(A1)),[112] which can be associated with the expression of key genes in osteoblast differentiation (Smad1, RUNX2 and OCN) (Fig. 4(A2)).[113]

In Xu's research work,[111] it was proven that a HAp-scaffold coated with polymeric materials can be established to overcome the issues associated with HAp low degradation. Since growth factors are adsorbed at the surface of the CaPs, its loading is limited. Coating the HAp structure with other materials can increase their incorporation as a result of increased surface area (more binding sites) and tuneable affinity (targeted binding enables a higher degree of growth factor attachment).[121,122] In this study, HAp porous scaffolds were coated with poly(L-lactide) (PLLA) fibers and supplemented with BMP-2 into the dorsal muscles of canines. The formation of bone was confirmed after a period of four weeks (Fig. 4(B3)). Similar results in a calvarial defect *in vivo* model were achieved by coating with ε-polycaprolactone (PCL),[123] or *in vitro* by modifying a HAp scaffold with collagen and BMP-2 conjugation.[124] The scaffold microstructure and resulting degradation rate can be manipulated by using biphasic calcium phosphate scaffolds, such as HAP/TCP systems.[125,126]

The use of polymeric matrixes in combination or incorporated with CaP particles is another route proposed to combine CaP with growth factors (Fig. 4(B)).[127] In the work of Li *et al.*,[114] a PCL scaffold with nano-HAp was coated with a polydopamine layer to facilitate covalent conjugation with BMP-2. The resulting material was used as a bone filler in rabbit calvaria defects *in vivo*, leading to substantial bone growth after 6 weeks and complete bone formation after 15 weeks (Fig. 4(B1)). In recent

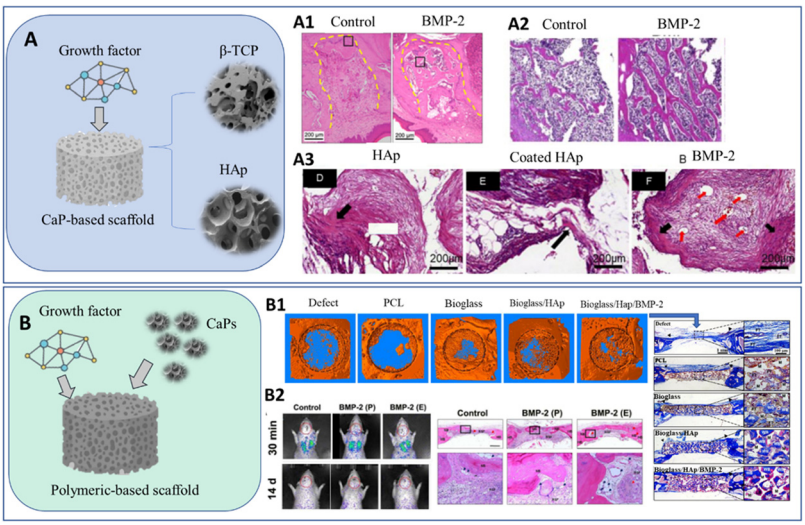

Fig. 4 Schematic representation of conventional CaP systems with growth factors using (A) β-TCP and HAp as structural scaffolds[12,111] and (B) applying other polymeric-based scaffolds loaded with CaP particles. Histology results after implantation: (A1) bone formation in tooth extraction sockets, 3 weeks after implantation;[112] (A2) bone formation 12 weeks after implantation in a femur bone defect;[113] (A3) bone and vessel formation (red arrows), 12 weeks after implanting in a subcutaneous model;[111] (B1) micro-CT and histology 6 weeks after implantation (blue and red represent immature bone matrix and maturing bone);[114] (B2) migration of BMSCs after injection of the biomaterial thought rat tail veins and bone formation after 12 weeks of implantation (BMP-2(P): scaffold with physically adsorbed BMP-2 and BMP-2 (E): scaffold with BMP-2 encapsulated into silk fibroin microspheres).[115]

studies, natural polymers such as silk fibroin have been explored for the same purpose, exhibiting sequential and sustained release of BMP-2 (Fig. 4(B2)).[115]

Although BMP-2/HAp composites have shown promising results in various *in vivo* studies, the intricate healing processes involved in bone tissue engineering may necessitate the inclusion of additional growth factors. Therefore, dual-releasing systems with melatonin (which modulates bone formation and resorption as it promotes the differentiation of osteoblast precursors toward osteoblasts),[128] SDF-1 (Stromal cell-derived factor-1) (which triggers the migration of stem cells and progenitor cells to injury sites during the acute phase of bone repair),[115] nerve growth factor (NGF) (regulating the functional attributes of central and peripheral neurons, such as development, differentiation, growth, and regeneration, which can effectively enhance osseointegration around implants),[129] TGF-β1 (Transforming growth factor beta) (causes induction of localized chondrogenesis when injected subperiosteally)[130] and platelet-derived growth factors (PDGF) (which increases the distance of cell infiltration into scaffolds)[131] have been reported to recreate natural biological cues.

The majority of published research on the incorporation of growth factors in bone tissue engineering has centered on BMP-2/vascular endothelial growth factor (VEGF) combinations. VEGF is known to play a role in the regulation of vascular development and angiogenesis, while also indirectly stimulating the differentiation of mesenchymal stem cells (MSCs) into the osteogenic lineage by inducing BMP-2 expression. Thus, the combination of BMP-2 and VEGF has been reported to obtain ceramic biomaterials with both osteogenic and angiogenic properties.[132,133] In fact, *in vitro* tests showed that dual systems have higher cell attachment and proliferation than HAp-based scaffolds with single growth factors;[134] while when implanted *in vivo*, it can benefit bone mineralization and expression of important bone matrix proteins.[135] Critical size defects in New Zealand white rabbits were also successfully treated using a DNA-loaded nano-CaP material with BMP and VEGF.[136]

3.2.2. Cell incorporation. The combination of HAp with MSCs can also be used as an approach to provide optimal performance in bone-tissue engineering, due to their ability to differentiate into osteoblasts or bone-forming cells. These cells can be isolated from different sources, such as human adipose-derived stem cells (ADSCs), which have the particularity of being largely available compared with other sources such as bone marrow and umbilical cord.[137] This incorporation is conventionally achieved by seeding the cells on top of the CaP scaffolds,[138,139] or by mixing particles with the cells prior to *in vitro* implantation or injection.[140,141]

Some studies report that the addition of these cells does not result in significant benefits in the enhancement of new bone formation *in vivo* models.[138,142] In the work of Supphaprasitt *et al.*,[138] although a PCL–biphasic-CaP scaffold seeded with ADSCs enhanced *in vitro* cell proliferation and differentiation, when implanted *in vivo* the results were similar to a cell-free scaffold.

However, according to recent developments in this field, CaP-based biomaterials in combination with cells can result in an enhanced clinical response. Brennan and co-authors[139] developed HAp and TCP scaffolds and showed that their bone formation capacity was highly increased with the addition of MSCs. The differences in the effects of the combinatory approach (cells-CaPs) can result in differences in microporosity and specific surface area, which ultimately lead to optimal cell invasion, interaction, and ingrowth.[139,143]

In addition to tailoring the CaP scaffold, the number of incorporated cells can affect the biological outcome. According to Mankani *et al.*,[140] the extent of bone formation can be improved by increasing the number of cells incorporated in the HAp/β-TCP system, and a minimal MSCs dose is required for optimal bone formation (between 0.3 and 1.0 million cells per 40 mg transplant).[140] Another approach includes the encapsulation of cells in degradable hydrogel microbeads in combination with CaP material.[141]

The combination of growth factors and cell incorporation can be used to develop next-generation therapeutic tools. In Overman's work,[144] a short pre-treatment with BMP-2 had a strong effect on the osteogenic differentiation of ADSCs seeded in a HAp/TCP (60/40) scaffold. Promoted osteodifferentiation was also reported by Zhao,[145] after the addition of BMP-2 in a HAp/TCP encapsulated with MSCs. In applications that require strong mechanical properties, such as spinal fusion defects in rabbits, BMP-2/cell systems can also enhance biomechanical stiffness, as a result of more rapid bone formation and consolidation.[146]

3.3. Conventional methodologies

Ion doping and growth factor incorporation in the context of a wet chemical precipitation process can involve different methodologies. In what concerns ion-doping, sequential precipitation, substitution during precipitation, ionic exchange, solid-state mixing, and impregnation are reported techniques in which the HAp particles are first formed and then a subsequent step is implemented to introduce the doping ions.[147,148] However, the controlled introduction of foreign ions into a material during precipitation, also known as co-nucleation doping, is the most common approach. In this process, a solution containing precursor components is mixed with another solution containing reactants under specific conditions. The precursor ions are then incorporated into the growing crystal lattice of the precipitate as the reaction proceeds. As the reaction progresses, new solid particles form and precipitate out of the solution.[149]

Stirred tank batch reactors and microreactors are used to carry out doped HAp synthesis.[150,151] However, doping ions can affect the nucleation and growth kinetics or crystallization dynamics, leading to alterations in the final morphology of HAp particles.[152,153] Hence, on one hand, the size and shape of the particles may be tuned by adjusting the concentration of the doping metal ions; on the other hand, it sets up an obstacle toward the production of HAp particles with the same morphology and size with different doping ratios.[152]

Bioactive factors can also be added to HAp through various techniques to functionalize the biomaterial for specific biological applications. In the adsorption method, growth factors can be adsorbed onto the surface of HAp particles by immersing the HAp particles in a solution containing the growth factor. The growth factor molecules adhere to the HAp surface due to electrostatic interactions and other binding forces.[154] Growth factors with charged regions can also be electrostatically attracted to HAp particles, leading to their adherence on the particle surfaces.[155] In addition, the inclusion of growth factors into coatings applied onto the surface of HAp particles is also possible using techniques like layer-by-layer deposition or spray coating.[156,157] Moreover, recent studies have encapsulated growth factors and cells in carriers, such as nanoparticles, microspheres, or hydrogels to protect the growth factors from degradation and provide controlled release when placed in contact with HAp or tissues.[158] In these processes, the reactor is used to produce HAp, which is then submitted to a post-processing step to introduce the growth factor.

Incorporation of growth factors during synthesis can also be achieved by incorporating them directly into the solution during the HAp precipitation process. According to the literature, the addition of growth factors can result in alterations in precipitation kinetics and the final particle's properties.[158,159]

4. HAp going 3D

Under physiological conditions, the tissues of the human body exhibit a complex 3D network structure. The development of alternative strategies that can accurately replicate the 3D anatomy and functions of tissues and organs remains a major challenge for bioengineers. The advancement of HAp-based scaffolds for clinical use necessitates a shift from traditional two-dimensional approaches towards more sophisticated 3D approaches. Additive manufacturing (AM) technologies provided hope for overcoming this critical challenge by allowing tailoring of the 3D scaffolds/implants in terms of: (1) shape; (2) architecture; (3) porosity; (4) pore interconnectivity; (5) material spatial distribution; (6) cell's spatial distribution; and, most importantly, (7) reduced fabrication times and reproducibility.[160] AM applied to tissue engineering and regenerative medicine presents a well-established workflow with 4 essential steps:

- Generation of the 3D model.
- 3D model processing in AM software.
- Produce the 3D scaffold by AM.
- 3D scaffold implantation (tissue replacement).

A vast number of materials have been processed by AM to produce HAp-based 3D scaffolds. HAp has been combined with several materials, both synthetic-based and natural-based materials, to develop suitable inks.[22] Inks require specific attributes that make them good contenders to be applied in AM strategies. These characteristics include suitable rheological properties such as viscosity, shear-thinning behavior, surface tension, *etc.*[161] However, it is important to consider the specific requirements and limitations of each AM technology when developing a HAp-based ink. Various AM technologies have been employed to fabricate such scaffolds, each with its own distinct requirements for the ink and a unique set of advantages and disadvantages. Nowadays, several 3D printed products incorporating HAp have been translated into the market. OsteoFab® is a 3D printed HAp-based implant that was developed by the medical technology division of the company 3D Systems. These implants are designed to assist

in bone regeneration and integration using a combination of polymer and HAp. OsteoFab® implants are created using additive manufacturing techniques, specifically 3D printing, which allows the production of patient-specific implants with complex geometries. The incorporation of HAp into the implant composition aims to enhance bone integration and promote long-term stability. MyBone®, the innovative product developed by Cerhum company, exhibits exceptional quality and remarkable efficacy in bone regeneration. This commercially available product has successfully promoted bone formation, highlighting its potential as a promising solution for bone tissue engineering applications.[162]

4.1. Additive manufacturing (AM)

The AM methods that can be applied for the fabrication of tissue engineered HAp-based 3D scaffolds can be divided into four main groups: inkjet-based, laser-based, extrusion-based and indirect-based.[163] The rheological properties of the ink have a significant impact on the success of the AM process, particularly with regards to the viscosity increase that is commonly imposed by the inclusion of HAp (more interactions within the ink, leading to increased viscosity and a thicker consistency). These challenges manifest in various forms, depending on the specific AM method employed (Table 3).

Table 3 Additive manufacturing techniques

Technique	Process	Description	Advantages	Disadvantages	Ref.
Inkjet-based techniques	Thermal	Inkjet thermal 3D printing, also referred to as ''Drop-on-Demand (DOD) 3D printing, uses an inkjet printhead to deposit droplets of a build material (often a photopolymer or a wax-like material) onto a build platform''. The droplets are expelled onto specific areas of the previous layer and are typically thermally cured or solidified to form a solid structure.	Speed and high resolution; multi-material printing; smooth surface finish.	Material limitations; post-processing required; size limitations.	164
	Piezoeletric	Inkjet piezoelectric 3D printing relies on piezoelectric crystals within the printhead. When an electrical voltage is applied to these crystals, they deform, causing a pressure wave that ejects a small droplet of material through a nozzle. The precise control over these piezoelectric actuators enables the deposition of materials in a highly controlled and precise manner.	Speed and high resolution; multi-material printing.	Material limitations; post-processing required; cost.	164
Laser-based techniques	Stereolithography (SLA)	SLA is one of the earliest and most widely used 3D printing technologies, known for its ability to produce high-resolution and highly detailed objects. It operates based on a process called photopolymerization using a UV laser or other light sources to selectively solidify a liquid photopolymer resin layer by layer.	Speed and high resolution.	Material limitations; post-processing required; cost.	165
	Selective laser sintering (SLS)	SLS is a powerful and versatile additive manufacturing technique known for its ability to produce strong, functional, and complex 3D-printed objects from a variety of materials. SLS employs a high-power laser to fuse powdered materials layer by layer.	Material versatility; geometry complexity; multi-part/object printing.	Surface finish; post processing required; material cost.	166
Extrusion-based techniques	Fused deposition modeling (FDM)	FDM is one of the most popular and accessible 3D printing techniques, known for its simplicity, versatility, and affordability. FDM works by melting and extruding a thermoplastic filament through a heated nozzle, which deposits the material layer by layer to build a three-dimensional object.	Affordability; material versatility; easy to use.	Surface finish; low resolution.	167
	Robotcasting	Robotcasting is an innovative 3D printing technique that combines aspects of both 3D printing and robotics to create large-scale structures and objects. This technique is based on a combination of robotics and traditional 3D printing principles. It involves a robotic arm with an attached nozzle that extrudes a material using a mechanical or electromagnetic actuator in layers to build structures.	Speed, material versatility, design freedom.	Material limitations; complexity.	167
Indirect-based techniques	Indirect 3D printing	Indirect 3D printing refers to methods where a temporary or sacrificial mold is 3D printed and then used as a template for creating the final object through various manufacturing processes. These techniques are used for applications where traditional 3D printing may not be the most suitable or cost-effective choice.	Material versatility; smooth surface finish; cost-effectiveness.	Low design freedom; time-consuming: material waste.	166

Inkjet-based printing allows controlled manufacturing using a droplet-based approach. The presence of HAp in the ink formulation (high viscosity) can be a huge barrier and this method is mostly avoided since it is only compatible with low viscosity inks (<10 mPa s).[164,168] However, a considerable quantity of publications on the use of inkjet printing in the manufacture of ceramics, including HAp, have shown promising results.[168]

The laser-based method uses as a major component a laser beam that focuses on the ink to selectively sinter it or concentrates its energy to deposit the ink in the substrate (receiver surface).[165] In the first case, since the beam is focused directly in the ink, it is incompatible to use cell-laden HAp bioinks due to the high energy density employed. In contrast, when the beam is used to deposit a thick layer of ink on the receiver surface, the direct printing of cell-laden bioinks is enabled without significantly affecting its viability.[169]

The extrusion-based methods have been the most used and consensual among the scientific community as the most promising methods to fabricate HAp-based 3D scaffolds. These methods consist in dispensing the ink through a nozzle coupled to an extruder that is steered through a mechanical or electromagnetic actuator. The dispensing mechanism can use a robotic arm (robocasting) that moves in different coordinates (*X*; *Y*; *Z*) to deposit the ink. Robocasting allows the ink extrusion at low (*e.g.*, 15 °C) and high temperatures (*e.g.*, 90 °C) enabling the printing of a wide range of biomaterials, either cell-free or cell-laden.[167] In addition, robocasting allows the deposition of more than one ink within the 3D scaffold. Another extrusion-based method, referred to as fused deposition modeling (FDM), is limited in its application to synthetic-based HAp inks as it requires the material to be printed at high temperatures (140–250 °C) in a melted state.[170] Consequently, it is not suitable for printing bioinks containing living cells.

Finally, the indirect-based method consists in using the above-mentioned methods to produce personalized molds in which through mold-cast HAp-based materials can be treated to produce 3D scaffolds.[166] The advantage of this method relies on the non-dependence of viscosity to produce the scaffold. However, mold-cast processes that usually involve methods like freeze-drying or critical point drying, require a subsequent post-printing process that uses strong chemicals to remove or dissolve the mold. This additional step does not allow the use of cell-laden HAp-based bioinks, limiting the use of mold-cast processes in tissue engineering applications. Furthermore, despite being a fast-setting method, it only allows the fabrication of simplistic 3D scaffolds losing the full potential of the AM methods.

4.1.1. HAp incorporation in 3D printed structures. The incorporation of HAp into 3D-printed scaffolds can enhance their biocompatibility and osteoconductivity, allowing for improved bone regeneration and tissue repair. However, the high viscosity imposed by HAp can present challenges during the 3D printing process, particularly in extrusion-based methods such as fused deposition modeling. To overcome these challenges, various strategies have been employed, including the blend with both synthetic and natural-based materials and the utilization of HAp granulate.

The use of synthetic biomaterials has emerged as a promising strategy for incorporating HAp into 3D printed scaffolds for medical applications.[171] In the context of HAp-based 3D printed scaffolds, synthetic biomaterials can be utilized to enhance the biocompatibility and osteoconductivity of the scaffold, as well as to address the processing challenges posed by the high viscosity of HAp.[23,172] Furthermore, the composition and properties of synthetic biomaterials can be precisely controlled, allowing for fine-tuning of the mechanical and biological properties of the scaffold.

The incorporation of HAp into 3D printed scaffolds can also be achieved using natural biomaterials. These materials are commonly derived from vegetal or animal sources and are attractive for their biocompatibility and biodegradability.[173] When combined with HAp, natural biomaterials can provide the necessary mechanical properties for tissue regeneration and repair, while also promoting cell adhesion and proliferation. Additionally, the use of natural biomaterials can mitigate the challenges posed by the high viscosity of HAp, providing an alternative to the use of synthetic biomaterials while providing biological cues and a better biological environment for tissue engineering applications. However, it is important to note that the composition and properties of natural biomaterials can vary greatly, depending on the source and processing methods used.

The HAp production method can also influence the quality and suitability of HAp materials for 3D printing scaffolds. The most common methods used to produce HAp are: (1) sol–gel synthesis; (2) precipitation; and (3) mechanical milling. Each method has its unique characteristics and suitability for scaffold fabrication. Sol–gel synthesis transforms precursor solutions or gels into solid HAp through chemical reactions, yielding HAp powder known for its high purity and homogeneity.[63] However, this method is highly complex, time-consuming and the chemicals and equipment required for sol–gel synthesis can be expensive. Mechanical milling methods produce HAp powders with fine particle sizes and controlled properties.[171,174] This approach stands out because of its simplicity and cost-effectiveness. It offers good reproducibility, displaying high yields with easy management of reaction conditions. Moreover, it can be easily integrated into large-scale industrial processes.[37,175]

Despite being a method that allows control of the final particle size by tuning the process parameters, this can be a challenge and there is a high risk of particle agglomeration. Thus, continuous precipitation systems with improved liquid–solid transportation and enhanced mass-heat transfer[65,176] have been increasingly applied in both research and pharmaceutical companies.[20,177]

4.1.2. HAp combined with synthetic-based polymers. Polylactic acid (PLA) and HAp is a common combination used to produce 3D printed scaffolds for tissue engineering applications. PLA is a biodegradable and biocompatible polymer that can be processed into 3D printing filaments and used to

fabricate scaffolds with controlled pore size, porosity, and mechanical properties.[178] The combination of PLA and HAp in 3D printed scaffolds offers a number of advantages, including improved mechanical strength, biocompatibility, and osteoconductivity. Russias *et al.*,[179] developed PLA-based constructs reinforced with HAp powder using an extrusion-based 3D printing approach. The 3D structures were successfully printed using ink composed of 70% HAp. The scaffolds presented suitable porosity (~55%) and acceptable mechanical performance with values of elastic modulus ranging from 84 to 150 MPa. The mechanical properties are still far from the minimal requirements for bone applications and in this study no biological tests were performed. The incorporation of natural-based biomaterials in combination with PLA and HAp to produce 3D printed structures has shown promising biological outcomes in terms of cell attachment and proliferation. Additionally, 3D-printed PLA/HAp scaffolds that combine the benefits of antimicrobial and bone regeneration properties have been developed and tested *in vivo* (Fig. 5(A)).[180] The results showed that the 3D-printed scaffold effectively inhibited bacterial growth and promoted bone regeneration in infected bone defect models. Additionally, the scaffold provided a suitable environment for bone cell proliferation and differentiation, leading to improved bone regeneration.

Poly(L-lactic) acid (PLLA) has also been used to develop printed HAp structures. Shuai and co-authors blended PGA into a HAp/PLLA scaffold by laser 3D printing to accelerate degradation, owing to the degradation of high hydrophilic PGA and the subsequent accelerated hydrolysis of PLLA chains. The developed 3D construct exhibited good osteoblast adhesion, spreading and proliferation of MG-63 human osteoblast-like cells. *In vivo*, when used in bone defects in New Zealand white rabbits, the scaffolds resulted in bone defect repair and blood vessel tissue formation after 8 weeks of implantation.[181] In another study, the authors blended PLLA with Hap-graphene oxide (GO), in which the oxygen-containing groups in GO served as anchor sites for the chelation of Ca^{2+} and then Ca^{2+} absorbed HPO_4^{2-} *via* electrovalent bonding to form homogeneously dispersed HAp nanorods[182] The resulting scaffolds exhibited good bioactivity by inducing the formation of an apatite layer and increased viability of MG-63 after 5 days of cell culture. Moreover, the incorporation of HAp-GO improved the compressive properties of the PLLA scaffold.

Another common synthetic polymer used in combination with HAp is polycaprolactone (PCL), a biodegradable and biocompatible polymer that has been widely used in the fabrication of 3D printed scaffolds due to its good mechanical properties and ability to degrade into non-toxic by-products.[183] Therefore, PCL has been combined with HAp to develop reinforced scaffolds employing different AM techniques. Recently, Petretta *et al.*,[184] developed and characterized 3D-printed magnetic scaffolds using a composite material made of PCL and HAp. The results showed that the addition of HAp to PCL improved the scaffold's mechanical properties, making it more suitable for use as a bone scaffold. The scaffolds exhibited good biodegradability and provided a supportive environment

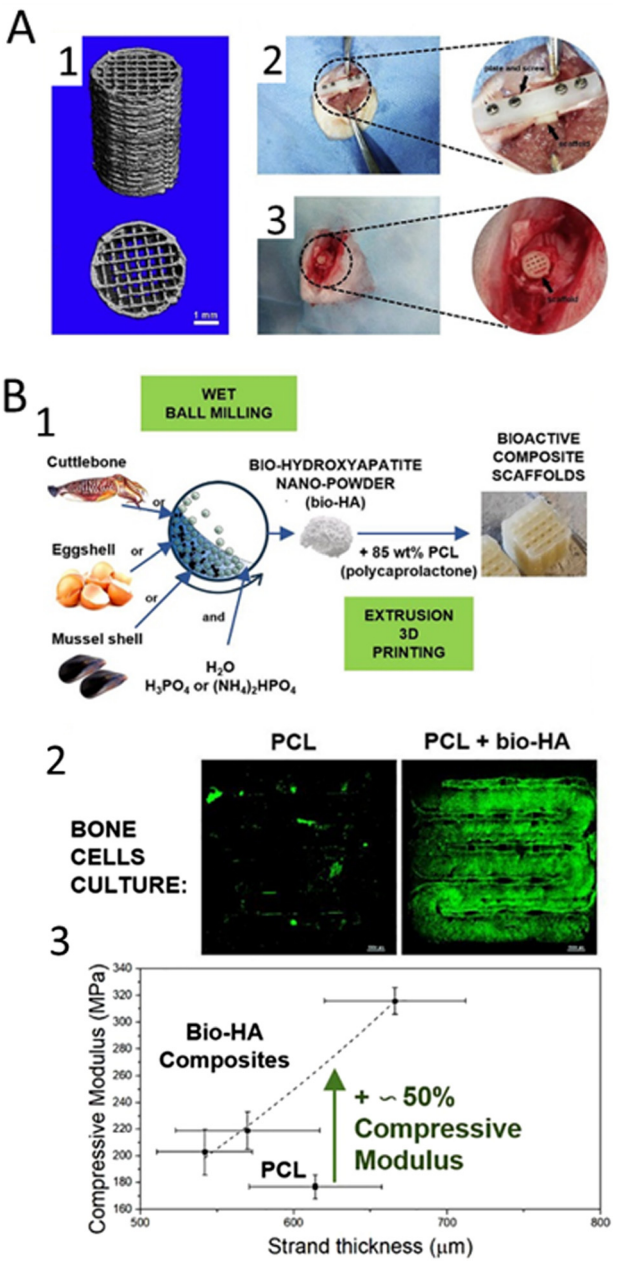

Fig. 5 Synthetic-based biomaterials incorporated with HAp used for 3D printing of scaffolds. (A) PLA/HAp 3D printed scaffold;[180] (A1) micro-CT reconstructed images of 3D-printed PLA/HAp scaffolds; (A2) femoral shaft critical segmental bone defect and (A3) femoral condyle local bone defect implanted with PLA/HAp scaffolds. (B) 3D-printed magnetic scaffolds using a composite material made of PCL and HAp.[185] (B1) Confocal images of the cells seeded on the PCL and PCL/HAp 3D printed scaffolds; (B2) compressive modulus *vs.* strand thickness curve of the PLC and PCL/HAp 3D printed scaffolds.

for the growth and proliferation of osteoblastic cells. Additionally, the addition of magnetic particles improved the MRI visibility of the scaffold, making it more suitable for tracking it *in vivo*. In another interesting work, the authors used HAp produced from biogenic sources[185] (Fig. 5(B1)). Again, the addition of HAp improved the biological and mechanical properties of the

scaffolds, making them more suitable for use as a bone scaffold (Fig. 5(B2)).

Another synthetic polymer that can be combined with HAp for the production of 3D printed scaffolds is poly(methyl methacrylate) (PMMA). PMMA is a synthetic polymer that is commonly used in a variety of medical and dental applications due to its transparency, toughness, and biocompatibility products.[186] PMMA-based polymers represent a group of resins commonly applied in clinics and are used for reconstructive surgery applications such as *in situ* formed bone cement or pre-surgically bone implant in the craniofacial area.[187,188] When used in 3D printing, PMMA can be processed into a fine powder or liquid and then fused into solid object layer-by-layer products. However, PMMA is not biodegradable, meaning that it does not degrade over time and may require removal once the tissue engineering process is complete. A conventional strategy to improve the overall biological activity and bone ingrowth properties, that allow the stabilization of the structure *in vivo* is the incorporation of HAp, encouraging better interactions with living tissues. A recent study showed that the incorporation of PCL surface-modified HAp into PMMA increased cell proliferation and mineralization as well as enhanced bone ingrowth properties of PMMA, as demonstrated by increased bone density and bone-to-implant contact[187] (Fig. 6). This study revealed that the modification of HAp particles with PCL is a promising alternative for bone regeneration. This combination has also been applied in 3D printing approaches and showed promising results.[188]

4.1.3. HAp combined with natural polymers. In contrast to synthetic polymers, natural-polymers are largely represented by hydrogel-based materials that are primarily processed through extrusion-based AM techniques. This results from the fact that they are typically either thermosetting or elastomeric in nature, therefore, not suitable for thermal processing. When dissolved and combined with HAp, they present a fluidic nature, being typically printed in a liquid-viscous state. After printing, a post-processing step is often required to enhance the long-term stability of the printed structures under physiological conditions. These procedures are highly dependent on the printed material and significant efforts have been made to identify the most suitable cross-linking strategy for each candidate material.

Furthermore, strong and stable interfacial bonding is essential to ensure that the composite material retains its mechanical integrity, biocompatibility, and functionality and is critical for the development of bioinks.[190] This interfacial bonding can be achieved by chemical bonding, physical interactions, cross-linking agents, or surface modifications, where the choice of the natural polymer, the method of processing, and the specific application will influence the type and strength of the interfacial bonding.[191,192]

The growing interest in printing HAp-reinforced natural-based biomaterials stems from the potential to simultaneously incorporate cells and/or bioactive molecules within the hydrogel matrix, in addition to HAp reinforcement, to promote cell proliferation/differentiation or elicit a desired *in vivo* response.[193]

Alginate is a natural polymer derived from brown seaweed and is commonly used in medical applications due to its biocompatibility and biodegradability. It has excellent gelation properties and can be easily processed into a gel-like substance, making it a suitable material for 3D printing.[194] The combination of alginate and HAp in 3D printed scaffolds offers several advantages, including improved biocompatibility, biodegradability, and osteoconductivity.[195]

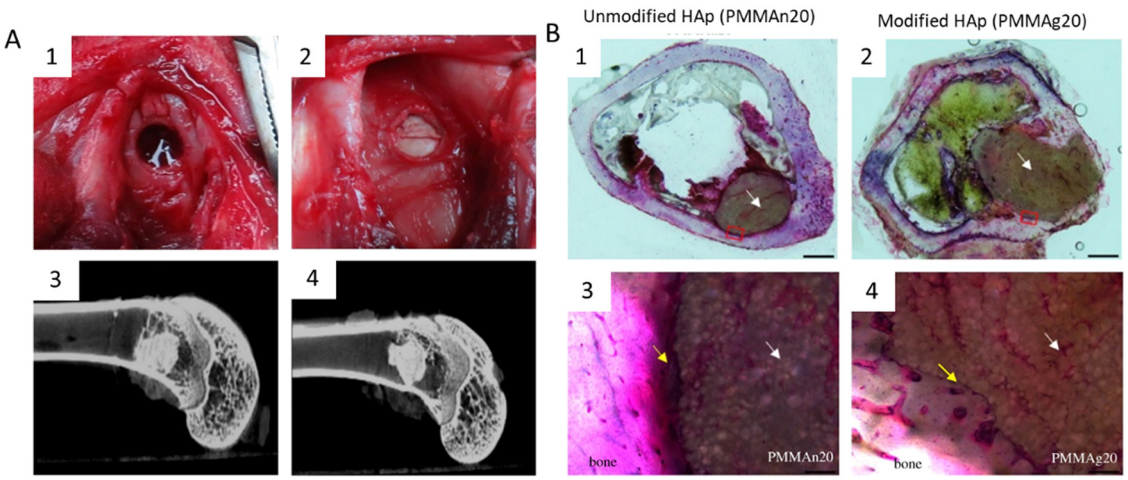

Fig. 6 HAp was modified with PCL and further incorporated into PMMA to improve the functionality of PMMA cement in bone regeneration.[189] (A) PMMA/HAp composites implanted into bone tissue. (A1) Appearance of the femoral condyle bone defect; (A2) PMMA/HAp composite implanted in the bone defect; (A3) micro CT image of the defect site after three months of being implanted with unmodified HAp; (A4) micro CT image of the defect site after three months of being implanted with modified HAp. (B) Histological images of bone tissue with the PMMA/HAp composite implanted for three months. (B1) and (B2) Histological images of bone after 3 months of PMMA incorporation with unmodified HAp and PCL modified HAp, respectively (scale bar 1 mm); (B3) and (B4) magnified images of the red squares on both composites, showing that the unmodified HAp composite was separated from the host bone by a layer of fibrous tissue (yellow arrow); whereas, HAp modified with PCL had a tight connection to the surrounding bone tissue, which revealed better bone ingrowth (scale bar 20 μm).

Alginate has also been used a bioink. Improved osteogenesis of stem cells encapsulated in HAp-reinforced alginate hydrogels has been proved due to alteration in DNA methylation with the consequent modification of gene expression of an osteogenic phenotype.[196] For instance, Wang *et al.*,[197] conducted a study that showed that human adipose-derived stem cells (hASCs) exhibited elevated expression of genes related to osteogenesis (OCN and RUNX2) in nano-HAp-loaded alginate hydrogels when compared to plain alginate hydrogels.[197]

Collagen is a natural protein that is also used with HAp to produce 3D printed scaffolds. This protein is widely found in the body, including in bones, skin, and connective tissues. It is biocompatible and has a similar composition to the extracellular matrix (ECM) of tissues, making it an attractive material for tissue engineering.[198] The main challenge in the fabrication of collagen/HAp scaffolds is the high viscosity of the composite. This can partially be addressed by using chemical solvents, but the use of solvents also makes it challenging to incorporate bioactive molecules.[198] As a result, the most widely pursued approach for producing collagen/HAp structures is indirect-based AM methods.[199] Lin *et al.*,[200] explored a novel approach to fabricate 3D constructs through the utilization of robocasting. The authors used a mixture of HAp and collagen to mimic the natural composition of bones and fabricate the scaffolds using a filament-free printing technique at a temperature of 4 °C. The resulting structures have a diameter range of 300–900 μm and are cross-linked using a genipin solution for stability. The results showed that the scaffolds produced using this technique show potential for use in bone regeneration applications due to their biomimetic composition and controlled structure.

Gelatin is a protein derived from collagen that has a gelling capacity and is often used in 3D printing. It is biocompatible and has been used in various biomedical applications, including as a scaffold material for 3D printing. This protein is water-soluble and presents several advantages mostly relying in the exposure of cell-ligand motifs (*i.e.*, RGD) that endorse cell adhesion to gelatin and target sequences for metalloproteinases (mitochondrial processing peptidase) that leads to *in vivo* enzymatic degradation and ECM remodeling.[201]

In the context of extrusion-based printing strategies, the control of temperature is generally required. Literature has described the printing of gelatin/HAp hydrogels by using a printing cartridge that is kept at a temperature greater than the sol–gel transition temperature and a printing plate with a controlled temperature that is lower than the sol–gel transition temperature. This is due to the fact that the thermoresponsive properties of gelatin hydrogels have been shown to not be affected by the addition of HAp.[202] Additionally, the addition of HAp to the ink has been demonstrated to enhance the rheological response as well as improving the structural properties of the printed scaffolds. The addition of HAp derivatives to the gelatin scaffold, as observed in other soft biocomposites such as alginate, has been shown to promote cell osteogenesis through increased expression of osteogenic genes and inorganic matrix deposition.[203] In the present study, gelatin was combined with decellularized bone particles (dbPTs, ~100 μm diameter) to produce 3D printed scaffolds. These scaffolds were further subjected to freeze-drying, and the obtained results revealed a decrease in pore size with an increase in HAp concentration (Fig. 7(A)). Additionally, the incorporation of dbPTs was revealed to slightly enhance the

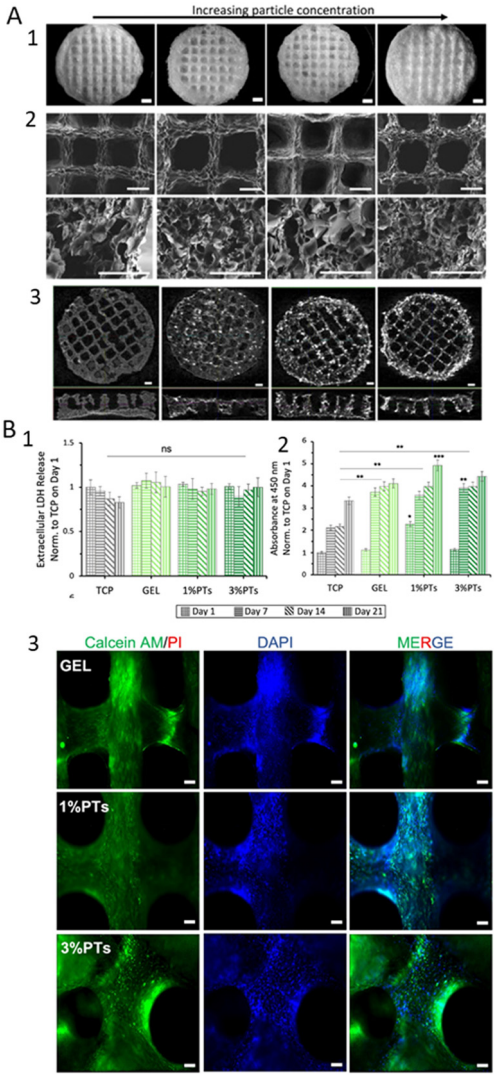

Fig. 7 Gelatin/dbPTs 3D printed scaffolds.[203] (A) Morphological analysis of the Gelatin/dbPTs 3D printed scaffolds. (A1) Light microscopy images of the scaffolds after freeze-drying (scale bars: 1 mm); (A2) SEM images of the scaffolds showing the surface morphology of the scaffolds on the top view and pore structure in the cross-sectional area (scale bars: 500 μm); (A3) micro CT cross-section image of the scaffolds (scale bar: 1 mm). (B) *In vitro* cytocompatibility assessment of the Gglatin/dbPTs 3D printed scaffolds. (B1) Quantification of the extracellular lactate dehydrogenase release assay (LDH) during 21 days of incubation; (B2) Cell viability assay of MC3T3-E1 cells on the Gelatin/dbPTs scaffolds (n = 6), statistically significant differences were determined between groups depending on each time point. All data are represented as mean ± SD. $^{**}p < 0.01$, $^{***}p < 0.001$ indicate a statistically significant difference among means; (B3) fluorescence microscopy images of MC3T3 cells on the scaffolds cultured for 14 days. Calcein AM (green), PI (red), DAPI (blue) staining represent live, dead cells and cell nuclei respectively (scale bars: 100 μm).

scaffolds biological properties in terms of LDH levels release and cell viability (Fig. 7(B)).

5. Conclusions and future perspectives

HAp is generated on a large scale annually to produce medical devices, and is widely used in bone and dental implants, as drug delivery systems, and tissue engineering. The industrialized batch production of this inorganic material is well-established, but there are still several drawbacks in conventional implemented methodologies to produce HAp and HAp composite particles, as well as complex 3D HAp-based structures.

Despite wet chemical precipitation being a method that allows the control of the final particle size by tuning the process parameters, batch operations can be a challenge and there is a high risk of particle agglomeration and wide distribution of properties. Thus, continuous precipitation systems with improved liquid–solid transportation and enhanced mass and heat transfer[65,176] have been increasingly applied by both research and pharmaceutical companies.[20,177]

As demonstrated in this review, new methodologies are being developed to improve reproducibility and scalability, such as continuous processes in microreactors and meso-oscillatory flow devices. These processes allow for efficient utilization of reagents, precise control over operating parameters, and consistent product quality with a smaller facility footprint, while being more energy-efficient due to reduced empty-fill and heat-up cycles.

In addition to guaranteeing the production of high-quality HAp, researchers are also focusing on enhancing the biological response of the resulting materials. Ion-doping, the combination with bioactive factors and the development of composite systems can enhance HAp's biological activity. As discussed in the present review these strategies can address some of the limitations of HAp in tissue engineering applications, by improving its mechanical properties, stability, cell response and antimicrobial activity. Several ions have been shown to enhance osteogenic activity, such as strontium and zinc. On the other hand, ions such as fluoride, silver, and copper have been used for their antimicrobial properties. From a bone tissue engineering viewpoint, incorporating bioactive factors in HAp is a common approach. Growth factors like BMP-2 play a crucial role in promoting osteogenesis and chondrogenesis. The simplest method involves the adsorption of BMP-2 onto HAp scaffolds or particles. Another approach is combining HAp with growth factors using polymeric matrices. Dual-releasing systems with multiple growth factors, such as BMP-2/VEGF combinations, have shown promising results in promoting bone formation and angiogenesis. Cell incorporation, particularly mesenchymal stem cells (MSCs), in HAp-based scaffolds can enhance bone formation. Combining growth factors and cell incorporation can lead to improved bone tissue engineering outcomes leading to next generation biotherapies.

In the context of ion-doping and incorporation of bioactive factor, MOFPRemerges as an optimal system for the continuous production of doped HAp particles, particularly within the scope of biomaterial synthesis for tissue engineering purposes. The micromixing efficiency, diminished shear stress, and improved suspension of solids of this system ensure the synthesis of homogeneous particles and can enhance the uniform integration of dopant ions throughout the HAp lattice.[14,34] Moreover, this reactor offers the possibility of controlling the final physicochemical properties (such as crystallinity, mean particle size, particle size distribution and morphology) using the oscillation frequency and amplitude.[14,70] In addition, the doping ions may form impurity phases during the growth of HAp nanocrystals.[152] According to published data, the use of meso-OFR for HAp precipitation can reduce the reaction time by four times while avoiding the formation of intermediate CaPs phases.[17,19]

Thus, changing the oscillatory flow conditions in oscillatory flow-based reactors can open new avenues in the development of tailored HAp-growth factor particles by allowing better control over nucleation and crystal growth rates.[204] Given the necessity of balancing optimization with the preservation of HAp structure, the thorough control provided by this type of reactor can be particularly advantageous. This technology can play a role in bridging the gap between academic exploration and large-scale industrial production, presenting an adaptable foundation for the consistent fabrication of composite HAp particles on a large scale.

The produced HAp and HAp composites can be further used to develop complex 3D structures. AM-based technology, particularly 3D printing and bioprinting are currently the most cutting-edge approaches. These processes have shown high potential in tissue engineering by allowing for customized patient-specific structures and grafts, with successful outcomes in regenerating hard tissues using tissue-specific printed constructs.

The choice of HAp production method should rely on various considerations, including the intended application, desired particle characteristics, and compatibility with additive manufacturing technologies. In these technologies, methods that generate HAp powders with fine particles, high purity, and suitable rheological properties are preferred. Firstly, HAp particle size and size distribution are essential for even distribution during 3D printing processes like stereolithography (SLA) and selective laser sintering (SLS).[205,206] Inconsistent particle sizes or aggregates produced by certain methods can lead to printing difficulties and result in uneven scaffold structures. Secondly, the rheological properties of HAp suspensions or pastes, such as viscosity and shear-thinning behavior, influence extrusion-based methods like fused deposition modeling and robocasting.[207] These properties are sensitive to the production method used, necessitating tailored HAp formulations for specific 3D printing techniques. In this context, continuous synthesis approaches, in particular oscillatory flow technology, can reduce the particle size distribution and particle aggregation degree, improving process reproducibility.[17,28]

Moreover, the control over the operation parameters (such as frequency (f) and amplitude (x_0) oscillation, residence time (τ)), allows optimization of the final physicochemical and rheological properties. Thus, this methodology is particularly well-suited for producing HAp powders for 3D printing.[32,208,209] Furthermore, binder materials, employed in methods like inkjet printing, interact with HAp and affect scaffold mechanical strength and porosity.[210]

Regarding the effect of HAp concentration in printed biomaterials, higher HAp concentration often enhances the mechanical strength and structural integrity of printed constructs, making the printed structures more robust and capable of mimicking natural tissues.[211,212] However, high concentrations typically increase the viscosity of the HAp suspension[207] and can also negatively impact the biological activity due to changes in pH, osmolarity, and ion concentrations.[212] While HAp is often considered biocompatible, high calcium concentrations might trigger unwanted immune responses or affect interactions between cells and the substrate.[175] Moreover, high concentrations can lead to nozzle clogging or other printing issues, affecting print resolution and accuracy.[213]

In summary, it all comes down to obtaining HAp particles with specific properties (*i.e.* applying a synthesis methodology and a reactor that allow for greater particle control, reproducibility, and scale-up) so that these can be used in 3D printing, and according to the application combined with other materials, and optimized to match the desired properties. However, there is still a long way to go, since HAp particles and composites utilized in 3D printing applications are acquired through commercial sources rather than in-house production. Current works fail to address these issues and optimize HAp particles in the development of new biomaterials.

Appropriate optimization of inks/bioink design and development is crucial for native-like tissue regeneration, including implant integration, remodeling, vascularization, and maturation. Understanding biomaterials, cells, printing methods, and the *in vivo* environment is necessary. Printing more complex architectures with multiple materials and cell types for *in vivo* cellular diversity and functionality is also an opportunity to better meet the native tissue but it brings new technical barriers that will take time to overcome.

Finally and due to the increasing demand for HAp in biomedical applications, it is crucial to explore in the future the natural and renewable resources for this bioceramic. Thus, extracting HAp from a natural source could alleviate the problem of producing synthetic HAp. Animal bones and scales, for instances, can be a good source for producing HAp, ensuring sustainability, allowing for nutrient recovery of waste materials transforming them into added value materials.

Studying and comprehending the properties of HAp, such as phase purity and thermal stability, as well as enhancing extraction processes, are crucial steps in guaranteeing the ultimate quality of the obtained HAp. These measures are critical for the successful introduction of bio-HAp to the market as a dependable bioceramic suitable for medical applications.

Author contributions

A. V: conceptualization, writing – original draft; S. M.: writing – original draft; J. B. C: conceptualization, writing – original draft, review & editing; F. C: writing – review & editing, supervision, validation; F. R: writing – review & editing, supervision, validation; A. L. O: conceptualization, supervision, writing – review & editing, validation.

Conflicts of interest

There are no conflicts to declare.

Acknowledgements

This work was financially supported by: National Funds through FCT (Foundation for Science and Technology) under the project UIDB/50016/2020 of the Centre for Biotechnology and Fine Chemistry – CBQF; and by LA/P/0045/2020 (ALiCE), UIDB/00511/2020 and UIDP/00511/2020 (LEPABE), funded by national funds through FCT/MCTES (PIDDAC). A. Veiga gratefully acknowledges doctoral scholarship [2020.08683.BD] from FCT. Joao B. Costa would like to acknowledge FCT—Fundação para a Ciência e a Tecnologia, I.P. and, when eligible, by COMPETE 2020 FEDER funds, under the Scientific Employment Stimulus—Individual Call (CEEC Individual) – 2022.02781.CEECIND – "MOTION: Multi-biofabrication of patient-specific tissues for regeneration of knee meniscus". Filipa Castro acknowledges FCT CEEC Individual contract (2022.06818.CEECIND).

References

1 N. W. Kucko, R.-P. Herber, S. C. G. Leeuwenburgh and J. A. Jansen, Calcium Phosphate Bioceramics and Cements, *Principles of Regenerative Medicine*, Elsevier, 2019, pp.591–611, DOI: 10.1016/B978-0-12-809880-6.00034-5.

2 J. Jeong, J. H. Kim, J. H. Shim, N. S. Hwang and C. Y. Heo, Bioactive calcium phosphate materials and applications in bone regeneration, *Biomater. Res.*, 2019, **23**(1), 4, DOI: 10.1186/s40824-018-0149-3.

3 S. Kuttappan, D. Mathew and M. B. Nair, Biomimetic composite scaffolds containing bioceramics and collagen/gelatin for bone tissue engineering – A mini review, *Int. J. Biol. Macromol.*, 2016, **93**, 1390–1401, DOI: 10.1016/j.ijbiomac.2016.06.043.

4 R. Leu Alexa, *et al.*, 3D Printed Composite Scaffolds of GelMA and Hydroxyapatite Nanopowders Doped with Mg/Zn Ions to Evaluate the Expression of Genes and Proteins of Osteogenic Markers, *Nanomaterials*, 2022, **12**(19), 3420, DOI: 10.3390/nano12193420.

5 M. Ito, Y. Hidaka, M. Nakajima, H. Yagasaki and A. H. Kafrawy, Effect of hydroxyapatite content on physical properties and connective tissue reactions to a chitosan-hydroxyapatite composite membrane, *J. Biomed. Mater. Res.*, 1999, **45**(3), 204–208, DOI: 10.1002/(sici)1097-4636(19990605)45:3<204::aid-jbm7>3.0.co;2-4.

6 M. Bohner, L. Galea and N. Doebelin, Calcium phosphate bone graft substitutes: Failures and hopes, *J. Eur. Ceram. Soc.*, 2012, **32**(11), 2663–2671, DOI: **10.1016/j.jeurceramsoc.2012.02.028**.

7 M. B. Nair, H. K. Varma and A. John, Triphasic ceramic coated hydroxyapatite as a niche for goat stem cell-derived osteoblasts for bone regeneration and repair, *J. Mater. Sci.: Mater. Med.*, 2009, **20**(Suppl. 1), 809–812, DOI: **10.1007/s10856-008-3598-8**.

8 G. With, H. J. A. Dijk, N. Hattu and K. Prijs, Preparation, microstructure and mechanical properties of dense polycrystalline hydroxy apatite, *J. Mater. Sci.*, 1981, **16**(6), 1592–1598, DOI: **10.1007/bf00553971**.

9 L. Chen, J. Hu, J. Ran, X. Shen and H. Tong, A novel nanocomposite for bone tissue engineering based on chitosan–silk sericin/hydroxyapatite: biomimetic synthesis and its cytocompatibility, *RSC Adv.*, 2015, **5**(69), 56410–56422, DOI: **10.1039/C5RA08216A**.

10 M.-J. Kim and S. Choe, BMPs and their clinical potentials, *BMB Rep.*, 2011, **44**(10), 619–634, DOI: **10.5483/BMBRep.2011.44.10.619**.

11 J. C. Elliott, *Structure and Chemistry of the Apatites and Other Calcium Orthophosphates*, Elsevier Science, Amsterdam, 1st edn, 1994, vol. 18.

12 J. Sohier, G. Daculsi, S. Sourice, K. de Groot and P. Layrolle, Porous beta tricalcium phosphate scaffolds used as a BMP-2 delivery system for bone tissue engineering, *J. Biomed. Mater. Res., Part A*, 2010, **92**(3), 1105–1114, DOI: **10.1002/jbm.a.32467**.

13 F. Castro, *et al.*, Process intensification and optimization for hydroxyapatite nanoparticles production, *Chem. Eng. Sci.*, 2013, **100**, 352–359, DOI: **10.1016/j.ces.2013.01.002**.

14 A. Veiga, F. Castro, A. Ferreira, A. L. Oliveira and F. Rocha, Fabrication of calcium phosphates with controlled properties using a modular oscillatory flow reactor, *Chem. Eng. Res. Des.*, 2022, **183**, 90–103, DOI: **10.1016/j.cherd.2022.04.036**.

15 G. Gecim, S. Dönmez and E. Erkoc, Calcium deficient hydroxyapatite by precipitation: Continuous process by vortex reactor and semi-batch synthesis, *Ceram. Int.*, 2021, **47**(2), 1917–1928, DOI: **10.1016/j.ceramint.2020.09.020**.

16 F. Castro, Process Intensification for the production of hydroxyapatite nanoparticles, *Tese de Doutoramento na Escola de Engenharia da Universidade do Minho*, 2013.

17 F. Castro, A. Ferreira, F. Rocha, A. Vicente and J. A. Teixeira, Continuous-Flow Precipitation of Hydroxyapatite at 37 °C in a Meso Oscillatory Flow Reactor, *AIChE J.*, 2013, **59**(12), 4483–4493, DOI: **10.1002/aic.14193**.

18 J. F. Gomes, C. C. Granadeiro, M. A. Silva, M. Hoyos, R. Silva and T. Vieira, An Investigation of the Synthesis Parameters of the Reaction of Hydroxyapatite Precipitation in Aqueous Media, *Int. J. Chem. React. Eng.*, 2008, **6**, 1, DOI: **10.2202/1542-6580.1778**.

19 A. Veiga, F. Castro, A. Oliveira and F. Rocha, High efficient strategy for the production of hydroxyapatite/silk sericin nanocomposites, *J. Chem. Technol. Biotechnol.*, 2021, **96**(1), 241–248, DOI: **10.1002/jctb.6532**.

20 S. L. Lee, *et al.*, Modernizing Pharmaceutical Manufacturing: from Batch to Continuous Production, *J. Pharm. Innov.*, 2015, **10**(3), 191–199, DOI: **10.1007/s12247-015-9215-8**.

21 A. L. Zydney, Perspectives on integrated continuous bioprocessing—opportunities and challenges, *Curr. Opin. Chem. Eng.*, 2015, **10**, 8–13, DOI: **10.1016/j.coche.2015.07.005**.

22 A. Kumar, S. Kargozar, F. Baino and S. S. Han, Additive Manufacturing Methods for Producing Hydroxyapatite and Hydroxyapatite-Based Composite Scaffolds: A Review, *Front. Mater.*, 2019, **6**, DOI: **10.3389/fmats.2019.00313**.

23 Y. Kim, E.-J. Lee, A. P. Kotula, S. Takagi, L. Chow and S. Alimperti, Engineering 3D Printed Scaffolds with Tunable Hydroxyapatite, *J. Funct. Biomater.*, 2022, **13**(2), 34, DOI: **10.3390/jfb13020034**.

24 A. Veiga, F. Castro, C. C. Reis, A. Sousa, A. L. Oliveira and F. Rocha, Hydroxyapatite/sericin composites: A simple synthesis route under near-physiological conditions of temperature and pH and preliminary study of the effect of sericin on the biomineralization process, *Mater. Sci. Eng., C*, 2020, **108**, 110400, DOI: **10.1016/j.msec.2019.110400**.

25 S. Recillas, V. Rodríguez-Lugo, M. L. Montero, L. Hernandez, V. Castaño and C. Ricas, Studies on the precipitation behavior of calcium phosphate solutions, *J. Ceram. Process. Res.*, 2012, **13**(1), 5–10, [Online]. Available: **https://jcpr.kbs-lab.co.kr/file/JCPR_vol.13_2012/JCPR13-1/5_10.pdf**.

26 A. Yelten-Yilmaz and S. Yilmaz, Wet chemical precipitation synthesis of hydroxyapatite (HA) powders, *Ceram. Int.*, 2018, **44**(8), 9703–9710, DOI: **10.1016/j.ceramint.2018.02.201**.

27 F. Castro, A. Ferreira, F. Rocha, A. Vicente and J. António Teixeira, Characterization of intermediate stages in the precipitation of hydroxyapatite at 37 °C, *Chem. Eng. Sci.*, 2012, **77**(2), 150–156, DOI: **10.1016/j.ces.2012.01.058**.

28 F. Castro, *et al.*, Continuous-flow precipitation of hydroxyapatite in ultrasonic microsystems, *Chem. Eng. J.*, 2013, **215–216**, 979–987, DOI: **10.1016/j.cej.2012.11.014**.

29 F. Castro, A. Ferreira, F. Rocha, A. Vicente and J. A. Teixeira, Precipitation of hydroxyapatite at 37 °C in a meso oscillatory flow reactor operated in batch at constant power density, *AIChE J.*, 2013, **59**(12), 4483–4493, DOI: **10.1002/aic.14193**.

30 S. S. A. Abidi and Q. Murtaza, Synthesis and Characterization of Nano-hydroxyapatite Powder Using Wet Chemical Precipitation Reaction, *J. Mater. Sci. Technol.*, 2014, **30**(4), 307–310, DOI: **10.1016/j.jmst.2013.10.011**.

31 S. Mondal, A. Dey and U. Pal, Low temperature wet-chemical synthesis of spherical hydroxyapatite nanoparticles and their in situ cytotoxicity study, *Adv. Nano Res.*, 2016, **4**(4), 295–307, DOI: **10.12989/anr.2016.4.4.295**.

32 F. Castro, *et al.*, Continuous-flow precipitation as a route to prepare highly controlled nanohydroxyapatite: *in vitro* mineralization and biological evaluation, *Mater. Res. Express*, 2016, **3**(7), 075404, DOI: **10.1088/2053-1591/3/7/075404**.

33 J. Latocha, M. Wojasiński, P. Sobieszuk and T. Ciach, Synthesis of hydroxyapatite in a continuous reactor: A review, *Chem. Process Eng.*, 2018, **39**(3), 281–293, DOI: 10.24425/122950.

34 P. Cruz, C. Silva, F. Rocha and A. Ferreira, The axial dispersion of liquid solutions and solid suspensions in planar oscillatory flow crystallizers, *AIChE J.*, 2019, **65**(9), e16683, DOI: 10.1002/aic.16683.

35 F. Almeida, F. Rocha and A. Ferreira, Analysis of liquid flow and mixing in an oscillatory flow reactor provided with 2d smooth periodic constrictions, *J. Eng.*, 2018, **4**(2), 1–15, DOI: 10.24840/2183-6493_004.002_0001.

36 S. Liu, Ideal Flow Reactors, *Bioprocess Engineering*, Elsevier, 2017, pp.179–257, DOI: 10.1016/B978-0-444-63783-3.00005-8.

37 G. P. Demopoulos, Aqueous precipitation and crystallization for the production of particulate solids with desired properties, *Hydrometallurgy*, 2009, **96**(3), 199–214, DOI: 10.1016/j.hydromet.2008.10.004.

38 A. Monballiu, E. Desmidt, K. Ghyselbrecht and B. Meesschaert, Phosphate recovery as hydroxyapatite from nitrified UASB effluent at neutral pH in a CSTR, *J. Environ. Chem. Eng.*, 2018, **6**(4), 4413–4422, DOI: 10.1016/j.jece.2018.06.052.

39 K. Usami, K. Xiao and A. Okamoto, Efficient Ketose Production by a Hydroxyapatite Catalyst in a Continuous Flow Module, *ACS Sustainable Chem. Eng.*, 2019, **7**(3), 3372–3377, DOI: 10.1021/acssuschemeng.8b05574.

40 J. Gómez-Morales, J. Torrent-Burgués, T. Boix, J. Fraile and R. Rodríguez-Clemente, Precipitation of stoichiometric hydroxyapatite by a continuous method, *Cryst. Res. Technol.*, 2001, **36**(1), 15–26, DOI: 10.1002/1521-4079(200101)36:1<15::AID-CRAT15>3.0.CO;2-E.

41 A. Magrí, E. Company, F. Gich and J. Colprim, Hydroxyapatite Formation in a Single-Stage Anammox-Based Batch Treatment System: Reactor Performance, Phosphorus Recovery, and Microbial Community, *ACS Sustainable Chem. Eng.*, 2021, **9**(7), 2745–2761, DOI: 10.1021/acssuschemeng.0c08036.

42 A. Zoulalian and J. Villermaux, Influence of Chemical Parameters on Micromixing in a Continuous Stirred Tank Reactor, *Adv. Chem.*, 1975, **133**, 348–361, DOI: 10.1021/ba-1974-0133.ch027.

43 R. Zauner, *Scale-Up of Precipitation Processes*, PhD Thesis, Ramsay Memorial Laboratory of Chemical Engineering at University, London, 1994.

44 J. Chen and C. Zheng, Interaction of macro-and micromixing on particle size distribution in reactive precipitation, *Chem. Eng. Sci.*, 1996, **51**(10), 1957–1966.

45 K. Jähnisch, V. Hessel, H. Löwe and M. Baerns, Chemistry in Microstructured Reactors, *Angew. Chem., Int. Ed.*, 2004, **43**(4), 406–446, DOI: 10.1002/anie.200300577.

46 N. Jongen, *et al.*, Development of a Continuous Segmented Flow Tubular Reactor and the 'Scale-out' Concept – In Search of Perfect Powders, *Chem. Eng. Technol.*, 2003, **26**(3), 303–305, DOI: 10.1002/ceat.200390046.

47 J. Latocha, M. Wojasiński, K. Jurczak, S. Gierlotka, P. Sobieszuk and T. Ciach, Precipitation of hydroxyapatite nanoparticles in 3D-printed reactors, *Chem. Eng. Process.*, 2018, **133**, 221–233, DOI: 10.1016/j.cep.2018.10.001.

48 M. Wojasiński, J. Latocha, P. Liszewska, Ł. Makowski, P. Sobieszuk and T. Ciach, Scaled-Up 3D-Printed Reactor for Precipitation of Lecithin-Modified Hydroxyapatite Nanoparticles, *Ind. Eng. Chem. Res.*, 2021, **60**(35), 12944–12955, DOI: 10.1021/acs.iecr.1c02973.

49 E. Fujii, K. Kawabata, Y. Shirosaki, S. Hayakawa and A. Osaka, Fabrication of calcium phosphate nanoparticles in a continuous flow tube reactor, *J. Ceram. Soc. Jpn.*, 2015, **123**(1435), 101–105, DOI: 10.2109/jcersj2.123.101.

50 K. Kandori, T. Kuroda, S. Togashi and E. Katayama, Preparation of Calcium Hydroxyapatite Nanoparticles Using Microreactor and Their Characteristics of Protein Adsorption, *J. Phys. Chem. B*, 2011, **115**(4), 653–659, DOI: 10.1021/jp110441e.

51 L. D. Esposti, *et al.*, Calcium phosphate nanoparticle precipitation by a continuous flow process: A design of an experiment approach, *Crystals*, 2020, **10**(10), 1–17, DOI: 10.3390/cryst10100953.

52 Y. He, K. J. Kim and C. H. Chang, Segmented microfluidic flow reactors for nanomaterial synthesis, *Nanomaterials*, 2020, **10**(7), 1–21, DOI: 10.3390/nano10071421, MDPI AG.

53 M. Akram, A. Z. Alshemary, Y. F. Goh, W. A. Wan Ibrahim, H. O. Lintang and R. Hussain, Continuous microwave flow synthesis of mesoporous hydroxyapatite, *Mater. Sci. Eng., C*, 2015, **56**, 356–362, DOI: 10.1016/j.msec.2015.06.040.

54 L.-H. Fu, Y.-M. Xie, J. Bian, M.-G. Ma, C.-H. Tian and X.-J. Jin, Microwave-assisted rapid synthesis of lignocellulose/hydroxyapatite nanocomposites, *Mater. Lett.*, 2015, **159**, 51–53, DOI: 10.1016/j.matlet.2015.06.082.

55 J. Latocha, M. Wojasiński, P. Sobieszuk and T. Ciach, Synthesis of hydroxyapatite in a continuous reactor: A review, *Chem. Process Eng.*, 2018, **39**(3), 281–293, DOI: 10.24425/122950.

56 Q. Yang, *et al.*, High throughput methodology for continuous preparation of hydroxyapatite nanoparticles in a microporous tube-in-tube microchannel reactor, *Ind. Eng. Chem. Res.*, 2010, **49**(1), 140–147, DOI: 10.1021/ie9005436.

57 FLUIDINOVA, FLUIDINOVA HYDROXYAPATITE, 2021. https://www.fluidinova.com/(accessed Jul. 23, 2021).

58 C. M. Fonte, M. E. Leblebici, M. M. Dias and J. C. B. Lopes, The NETmix reactor: Pressure drop measurements and 3D CFD modeling, *Chem. Eng. Res. Des.*, 2013, **91**(11), 2250–2258, DOI: 10.1016/j.cherd.2013.07.014.

59 P. E. M. S. C. Laranjeira, NetMix Static Mixer – Modelling, CFD Simulation and Experimental Characterisation. 2005.

60 M. R. Mackley, K. B. Smith and N. P. Wise, The Mixing and Separation of Particle Suspensions Using Oscillatory Flow in Baffled Tubes, *Chem. Eng. Res. Des.*, 1993, **71**(Part A), 649–655.

61 P. Bianchi, J. D. Williams and C. O. Kappe, Oscillatory flow reactors for synthetic chemistry applications, *J. Flow Chem.*, 2020, **10**(3), 475–490, DOI: 10.1007/s41981-020-00105-6.

62 T. McGlone, N. E. B. Briggs, C. A. Clark, C. J. Brown, J. Sefcik and A. J. Florence, Oscillatory Flow Reactors

(OFRs) for Continuous Manufacturing and Crystallization, *Org. Process Res. Dev.*, 2015, **19**(9), 1186–1202, DOI: 10.1021/acs.oprd.5b00225.

63 P. Bianchi, J. D. Williams and C. O. Kappe, *Oscillatory flow reactors for synthetic chemistry applications*, 1981, DOI: 10.1007/s41981-020-00105-6/Published.

64 P. Cruz, C. Alvarez, F. Rocha and A. Ferreira, Tailoring the crystal size distribution of an active pharmaceutical ingredient by continuous antisolvent crystallization in a planar oscillatory flow crystallizer, *Chem. Eng. Res. Des.*, 2021, **175**, 115–123, DOI: 10.1016/j.cherd.2021.08.030.

65 N. M. Reis, *Novel Oscillatory Flow Reactors for Biotechnological Applications*, PhD thesis, School of Engineering of the University, Minho, 2006.

66 A. Ferreira, F. Rocha, J. Teixeira and F. Castro, *Modular oscillatory flow plate reactor*, WO 2017/175207 A1, 2017.

67 H. Wang, *et al.*, A review of process intensification applied to solids handling, *Chem. Eng. Process.*, 2017, **118**, 78–107, DOI: 10.1016/j.cep.2017.04.007.

68 A. Ferreira, F. Rocha, J. Teixeira and A. Vicente., *Apparatus for mixing improvement based on oscillatory flow reactors provided with smooth periodic constrictions*. *Int. Pat.*, WO 2015/056156 A1., PCT/IB2014/065273, 2014.

69 T. McGlone, N. E. B. Briggs, C. A. Clark, C. J. Brown, J. Sefcik and A. J. Florence, Oscillatory Flow Reactors (OFRs) for Continuous Manufacturing and Crystallization, *Org. Process Res. Dev.*, 2015, **19**(9), 1186–1202, DOI: 10.1021/acs.oprd.5b00225.

70 A. Veiga, *et al.*, Continuous Production of Highly Tuned Silk/Calcium-Based Composites: Exploring New Pathways for Skin Regeneration, *Molecules*, 2022, **27**(7), 2249, DOI: 10.3390/molecules27072249.

71 A. Veiga, F. Castro, F. Rocha and A. L. Oliveira, Protein-Based Hydroxyapatite Materials: Tuning Composition toward Biomedical Applications, *ACS Appl. Bio Mater.*, 2020, **3**(6), 3441–3455, DOI: 10.1021/acsabm.0c00140.

72 Q. Wang, *et al.*, Experimental and simulation studies of strontium/fluoride-codoped hydroxyapatite nanoparticles with osteogenic and antibacterial activities, *Colloids Surf., B*, 2019, **182**, 110359, DOI: 10.1016/j.colsurfb.2019.110359.

73 S. Panseri, *et al.*, Intrinsically superparamagnetic Fe-hydroxyapatite nanoparticles positively influence osteoblast-like cell behaviour, *J. Nanobiotechnol.*, 2012, **10**, 1–10, DOI: 10.1186/1477-3155-10-32.

74 T. M. Fernandes Patrício, *et al.*, Bio-inspired polymeric iron-doped hydroxyapatite microspheres as a tunable carrier of rhBMP-2, *Mater. Sci. Eng., C*, 2021, **119**, 111410, DOI: 10.1016/J.MSEC.2020.111410.

75 A. Ressler, A. Žužić, I. Ivanišević, N. Kamboj and H. Ivanković, Ionic substituted hydroxyapatite for bone regeneration applications: A review, *Open Ceram.*, 2021, **6**, 100122, DOI: 10.1016/j.oceram.2021.100122.

76 T. Baskaran, N. F. Mohammad, S. S. Md Saleh, N. F. Mohd Nasir and F. D. Mohd Daud, Synthesis Methods of Doped Hydroxyapatite: A Brief Review, *J. Phys.: Conf. Ser.*, 2021, **2071**(1), 012008, DOI: 10.1088/1742-6596/2071/1/012008.

77 N. C. Reger, A. K. Bhargava, I. Ratha, B. Kundu and V. K. Balla, Structural and phase analysis of multi-ion doped hydroxyapatite for biomedical applications, *Ceram. Int.*, 2019, **45**(1), 252–263, DOI: 10.1016/j.ceramint.2018.09.160.

78 H. Shi, Z. Zhou, W. Li, Y. Fan, Z. Li and J. Wei, Hydroxyapatite Based Materials for Bone Tissue Engineering: A Brief and Comprehensive Introduction, *Crystals*, 2021, **11**(2), 149, DOI: 10.3390/cryst11020149.

79 D. Predoi, *et al.*, Development of Iron-Doped Hydroxyapatite Coatings, *Coatings*, 2021, **11**(2), 186, DOI: 10.3390/COATINGS11020186.

80 X. Jiang, Y. Zhao, C. Wang, R. Sun and Y. Tang, Effects of physico-chemical properties of ions-doped hydroxyapatite on adsorption and release performance of doxorubicin as a model anticancer drug, *Mater. Chem. Phys.*, 2022, **276**, 125440, DOI: 10.1016/j.matchemphys.2021.125440.

81 A. Pal, P. Nasker, S. Paul, A. Roy Chowdhury, A. Sinha and M. Das, Strontium doped hydroxyapatite from Mercenaria clam shells: Synthesis, mechanical and bioactivity study, *J. Mech. Behav. Biomed. Mater.*, 2019, **90**, 328–336, DOI: 10.1016/j.jmbbm.2018.10.027.

82 S. Balakrishnan, *et al.*, Influence of iron doping towards the physicochemical and biological characteristics of hydroxyapatite, *Ceram. Int.*, 2021, **47**(4), 5061–5070, DOI: 10.1016/j.ceramint.2020.10.084.

83 Z. Zhao, M. Espanol, J. Guillem-Marti, D. Kempf, A. Diez-Escudero and M.-P. Ginebra, Ion-doping as a strategy to modulate hydroxyapatite nanoparticle internalization, *Nanoscale*, 2016, **8**(3), 1595–1607, DOI: 10.1039/C5NR05262A.

84 H. Maleki-Ghaleh, *et al.*, Effect of zinc-doped hydroxyapatite/graphene nanocomposite on the physicochemical properties and osteogenesis differentiation of 3D-printed polycaprolactone scaffolds for bone tissue engineering, *Chem. Eng. J.*, 2021, **426**, 131321, DOI: 10.1016/j.cej.2021.131321.

85 T.-D. T. Nguyen, Y.-S. Jang, M.-H. Lee and T.-S. Bae, Effect of strontium doping on the biocompatibility of calcium phosphate-coated titanium substrates, *J. Appl. Biomater. Funct. Mater.*, 2019, **17**(1), 228080001982651, DOI: 10.1177/2280800019826517.

86 S. Jose, *et al.*, Preparation and characterization of Fe doped *n*-hydroxyapatite for biomedical application, *Surf. Interfaces*, 2021, **25**, 101185, DOI: 10.1016/j.surfin.2021.101185.

87 E. Ungureanu, *et al.*, *In Vitro* Evaluation of Ag- and Sr-Doped Hydroxyapatite Coatings for Medical Applications, *Materials*, 2023, **16**(15), 5428, DOI: 10.3390/ma16155428.

88 I. Ullah, *et al.*, Mechanical, Biological, and Antibacterial Characteristics of Plasma-Sprayed (Sr,Zn) Substituted Hydroxyapatite Coating, *ACS Biomater. Sci. Eng.*, 2020, **6**(3), 1355–1366, DOI: 10.1021/acsbiomaterials.9b01396.

89 K. Thanigai Arul, J. Ramana Ramya and S. Narayana Kalkura, Impact of Dopants on the Electrical and Optical Properties of Hydroxyapatite, *Biomaterials*, IntechOpen, 2020, DOI: 10.5772/intechopen.93092.

90 M. A. Goldberg, *et al.*, The enhancement of hydroxyapatite thermal stability by Al doping, *J. Mater. Res. Technol.*, 2020, **9**(1), 76–88, DOI: 10.1016/j.jmrt.2019.10.032.

91 P. Kazimierczak, J. Golus, J. Kolmas, M. Wojcik, D. Kolodynska and A. Przekora, Noncytotoxic zinc-doped nanohydroxyapatite-based bone scaffolds with strong bactericidal, bacteriostatic, and antibiofilm activity, *Biomater. Adv.*, 2022, **139**, 213011, DOI: 10.1016/j.bioadv.2022.213011.

92 K. Sinulingga, M. Sirait, N. Siregar and M. E. Doloksaribu, Investigation of Antibacterial Activity and Cell Viability of Ag/Mg and Ag/Zn Co-doped Hydroxyapatite Derived from Natural Limestone, *ACS Omega*, 2021, **6**(49), 34185–34191, DOI: 10.1021/acsomega.1c05921.

93 Y. Li, D. Zhang, Z. Wan, X. Yang and Q. Cai, Dental resin composites with improved antibacterial and mineralization properties *via* incorporating zinc/strontium-doped hydroxyapatite as functional fillers, *Biomed. Mater.*, 2022, **17**(4), 045002, DOI: 10.1088/1748-605X/ac6b72.

94 Y. C. Liu, *et al.*, *In Vitro* Bioactivity and Antibacterial Activity of Strontium-, Magnesium-, and Zinc-Multidoped Hydroxyapatite Porous Coatings Applied *via* Atmospheric Plasma Spraying, *ACS Appl. Bio Mater.*, 2021, **4**(3), 2523–2533, DOI: 10.1021/ACSABM.0C01535/ASSET/IMAGES/LARGE/MT0C01535_0010.JPEG.

95 F. Manzoor, *et al.*, 3D Printed Strontium and Zinc Doped Hydroxyapatite Loaded PEEK for Craniomaxillofacial Implants, *Polymers*, 2022, **14**(7), 1376, DOI: 10.3390/polym14071376.

96 S. Jiang, *et al.*, Synergistic Effect of Micro-Nano-Hybrid Surfaces and Sr Doping on the Osteogenic and Angiogenic Capacity of Hydroxyapatite Bioceramics Scaffolds, *Int. J. Nanomed.*, 2022, **17**, 783–797, DOI: 10.2147/IJN.S345357.

97 S. Ray, *et al.*, Strontium and bisphosphonate coated iron foam scaffolds for osteoporotic fracture defect healing, *Biomaterials*, 2018, **157**, 1–16, DOI: 10.1016/J.BIOMATERIALS.2017.11.049.

98 H. W. Kim and Y. J. Kim, Effect of silicon or cerium doping on the anti-inflammatory activity of biphasic calcium phosphate scaffolds for bone regeneration, *Prog. Biomater.*, 2022, **11**(4), 421–430, DOI: 10.1007/s40204-022-00206-6.

99 N. Salam and I. R. Gibson, Lithium ion doped carbonated hydroxyapatite compositions: Synthesis, physicochemical characterisation and effect on osteogenic response *in vitro*, *Biomater. Adv.*, 2022, **140**, 213068, DOI: 10.1016/j.bioadv.2022.213068.

100 S. Zakhireh, K. Adibkia, Y. Beygi-Khosrowshahi and M. Barzegar-Jalali, Osteogenesis Promotion of Selenium-Doped Hydroxyapatite for Application as Bone Scaffold, *Biol. Trace Elem. Res.*, 2021, **199**(5), 1802–1811, DOI: 10.1007/S12011-020-02309-2/FIGURES/9.

101 V. Gaddam, V. Podarala, S. K. Rayaduram Venkata, S. L. Mukku, R. Devalam and B. Kundu, Multi-ion-doped nano-hydroxyapatite-coated titanium intramedullary pins for long bone fracture repair in dogs—Clinical evaluation, *J. Biomed. Mater. Res., Part B*, 2022, **110**(4), 806–816, DOI: 10.1002/jbm.b.34960.

102 A. A. Aly and M. K. Ahmed, Fibrous scaffolds of Ag/Fe co-doped hydroxyapatite encapsulated into polycaprolactone: Morphology, mechanical and *in vitro* cell adhesion, *Int. J. Pharm.*, 2021, **601**, 120557, DOI: 10.1016/j.ijpharm.2021.120557.

103 M. Wojcik, *et al.*, Biocompatible curdlan-based biomaterials loaded with gentamicin and Zn-doped nano-hydroxyapatite as promising dressing materials for the treatment of infected wounds and prevention of surgical site infections, *Biomater. Adv.*, 2022, **139**, 213006, DOI: 10.1016/j.bioadv.2022.213006.

104 X. Liu, *et al.*, Ba/Mg co-doped hydroxyapatite/PLGA composites enhance X-ray imaging and bone defect regeneration, *J. Mater. Chem. B*, 2021, **9**(33), 6691–6702, DOI: 10.1039/D1TB01080H.

105 L. Yang, *et al.*, Bioactive Sr^{2+}/Fe^{3+} co-substituted hydroxyapatite in cryogenically 3D printed porous scaffolds for bone tissue engineering, *Biofabrication*, 2021, **13**(3), 035007, DOI: 10.1088/1758-5090/ABCF8D.

106 K. Sinulingga, M. Sirait, N. Siregar and H. Abdullah, Synthesis and characterizations of natural limestone-derived nano-hydroxyapatite (HAp): a comparison study of different metals doped HAps on antibacterial activity, *RSC Adv.*, 2021, **11**(26), 15896–15904, DOI: 10.1039/D1RA00308A.

107 J. Dulińska-Litewka, A. Łazarczyk, P. Hałubiec, O. Szafrański, K. Karnas and A. Karewicz, Superparamagnetic Iron Oxide Nanoparticles-Current and Prospective Medical Applications, *Materials*, 2019, **12**(4), 617, DOI: 10.3390/MA12040617.

108 T. P. Ribeiro, F. J. Monteiro and M. S. Laranjeira, PEGylation of iron doped hydroxyapatite nanoparticles for increased applicability as MRI contrast agents and as drug vehicles: A study on thrombogenicity, cytocompatibility and drug loading, *Eur. Polym. J.*, 2020, **137**, 109934, DOI: 10.1016/J.EURPOLYMJ.2020.109934.

109 L. Sheikh, S. Sinha, Y. N. Singhababu, V. Verma, S. Tripathy and S. Nayar, Traversing the profile of biomimetically nanoengineered iron substituted hydroxyapatite: synthesis, characterization, property evaluation, and drug release modeling, *RSC Adv.*, 2018, **8**(35), 19389–19401, DOI: 10.1039/C8RA01539B.

110 A. Tampieri, *et al.*, Intrinsic magnetism and hyperthermia in bioactive Fe-doped hydroxyapatite, *Acta Biomater.*, 2012, **8**(2), 843–851, DOI: 10.1016/J.ACTBIO.2011.09.032.

111 T. Xu, L. Sheng, L. He, J. Weng and K. Duan, Enhanced osteogenesis of hydroxyapatite scaffolds by coating with BMP-2-loaded short polylactide nanofiber: A new drug loading method for porous scaffolds, *Regener. Biomater.*, 2019, **7**(1), 91–98, DOI: 10.1093/rb/rbz040.

112 A. Mikai, *et al.*, BMP-2/β-TCP Local Delivery for Bone Regeneration in MRONJ-Like Mouse Model, *Int. J. Mol. Sci.*, 2020, **21**(19), 7028, DOI: 10.3390/ijms21197028.

113 Z. Xie, *et al.*, The fast degradation of β-TCP ceramics facilitates healing of bone defects by the combination of BMP-2 and Teriparatide, *Biomed. Pharmacother.*, 2019, **112**, 108578, DOI: 10.1016/j.biopha.2019.01.039.

114 X. Li, *et al.*, Accelerating Bone Healing by Decorating BMP-2 on Porous Composite Scaffolds, *ACS Appl. Bio Mater.*, 2019, **2**(12), 5717–5726, DOI: 10.1021/acsabm.9b00761.

115 X. Shen, *et al.*, Sequential and sustained release of SDF-1 and BMP-2 from silk fibroin-nanohydroxyapatite scaffold for the enhancement of bone regeneration, *Biomaterials*, 2016, **106**, 205–216, DOI: 10.1016/j.biomaterials.2016.08.023.

116 S. Hiromoto, *et al.*, *In vivo* degradation and bone formation behaviors of hydroxyapatite-coated Mg alloys in rat femur, *Mater. Sci. Eng., C*, 2021, **122**, 111942, DOI: 10.1016/j.msec.2021.111942.

117 Y. Shu, *et al.*, Degradation *in vitro* and *in vivo* of β-TCP/MCPM-based premixed calcium phosphate cement, *J. Mech. Behav. Biomed. Mater.*, 2019, **90**, 86–95, DOI: 10.1016/j.jmbbm.2018.10.001.

118 S. Aunoble, D. Clément, P. Frayssinet, M. F. Harmand and J. C. Le Huec, Biological performance of a new β-TCP/PLLA composite material for applications in spine surgery: *In vitro* and *in vivo* studies, *J. Biomed. Mater. Res., Part A*, 2006, **78A**(2), 416–422, DOI: 10.1002/jbm.a.30749.

119 Y. Kuroiwa, *et al.*, Escherichia coli-derived BMP-2-absorbed β-TCP granules induce bone regeneration in rabbit critical-sized femoral segmental defects, *Int. Orthop.*, 2019, **43**(5), 1247–1253, DOI: 10.1007/s00264-018-4079-4.

120 T. Ohyama, Y. Kubo, H. Iwata and W. Taki, Beta-Tricalcium Phosphate Combined With Recombinant Human Bone Morphogenetic Protein-2: A Substitute for Autograft, Used for Packing Interbody Fusion Cages in the Canine Lumbar Spine, *Neurol. Med. Chir.*, 2004, **44**(5), 234–241, DOI: 10.2176/nmc.44.234.

121 J. Wu, *et al.*, Growth factors enhanced angiogenesis and osteogenesis on polydopamine coated titanium surface for bone regeneration, *Mater. Des.*, 2020, **196**, 109162, DOI: 10.1016/j.matdes.2020.109162.

122 S. P. B. Teixeira, R. M. A. Domingues, M. Shevchuk, M. E. Gomes, N. A. Peppas and R. L. Reis, Biomaterials for Sequestration of Growth Factors and Modulation of Cell Behavior, *Adv. Funct. Mater.*, 2020, **30**(44), 1909011, DOI: 10.1002/adfm.201909011.

123 B.-S. Kim, S.-S. Yang and C. S. Kim, Incorporation of BMP-2 nanoparticles on the surface of a 3D-printed hydroxyapatite scaffold using an ε-polycaprolactone polymer emulsion coating method for bone tissue engineering, *Colloids Surf., B*, 2018, **170**, 421–429, DOI: 10.1016/j.colsurfb.2018.06.043.

124 N. T. B. Linh, C. D. G. Abueva, D. W. Jang and B. T. Lee, Collagen and bone morphogenetic protein-2 functionalized hydroxyapatite scaffolds induce osteogenic differentiation in human adipose-derived stem cells, *J. Biomed. Mater. Res., Part B*, 2020, **108**(4), 1363–1371, DOI: 10.1002/jbm.b.34485.

125 S. J. Polak, S. K. L. Levengood, M. B. Wheeler, A. J. Maki, S. G. Clark and A. J. W. Johnson, Analysis of the roles of microporosity and BMP-2 on multiple measures of bone regeneration and healing in calcium phosphate scaffolds, *Acta Biomater.*, 2011, **7**(4), 1760–1771, DOI: 10.1016/j.actbio.2010.12.030.

126 M. Mohammadi Zerankeshi, S. Mofakhami and E. Salahinejad, 3D porous HA/TCP composite scaffolds for bone tissue engineering, *Ceram. Int.*, 2022, **48**(16), 22647–22663, DOI: 10.1016/j.ceramint.2022.05.103.

127 P. Rittipakorn, N. Thuaksuban, K. Mai-Ngam, S. Charoenla and W. Noppakunmongkolchai, Bioactivity of a novel polycaprolactone-hydroxyapatite scaffold used as a carrier of low dose bmp-2: An *in vitro* study, *Polymers*, 2021, **13**(3), 1–15, DOI: 10.3390/polym13030466.

128 H. Jarrar, D. Çetin Altındal and M. Gümüşderelioğlu, Scaffold-based osteogenic dual delivery system with melatonin and BMP-2 releasing PLGA microparticles, *Int. J. Pharm.*, 2021, **600**, 120489, DOI: 10.1016/j.ijpharm.2021.120489.

129 J. Ye, B. Huang and P. Gong, Nerve growth factor-chondroitin sulfate/hydroxyapatite-coating composite implant induces early osseointegration and nerve regeneration of peri-implant tissues in Beagle dogs, *J. Orthop. Surg. Res.*, 2021, **16**(1), 51, DOI: 10.1186/s13018-020-02177-5.

130 K. Hanada, *et al.*, BMP-2 Induction and TGF-b1 Modulation of Rat Periosteal Cell Chondrogenesis, 2001.

131 E. A. Bayer, *et al.*, Programmed platelet-derived growth factor-bb and bone morphogenetic protein-2 delivery from a hybrid calcium phosphate/alginate scaffold, *Tissue Eng., Part A*, 2017, **23**(23–24), 1382–1393, DOI: 10.1089/ten.tea.2017.0027.

132 T. W. Kim, *et al.*, Combined Delivery of Two Different Bioactive Factors Incorporated in Hydroxyapatite Microcarrier for Bone Regeneration, *Tissue Eng. Regener. Med.*, 2020, **17**(5), 607–624, DOI: 10.1007/s13770-020-00257-5.

133 Z. S. Patel, S. Young, Y. Tabata, J. A. Jansen, M. E. K. Wong and A. G. Mikos, Dual delivery of an angiogenic and an osteogenic growth factor for bone regeneration in a critical size defect model, *Bone*, 2008, **43**(5), 931–940, DOI: 10.1016/j.bone.2008.06.019.

134 M. Sukul, T. B. L. Nguyen, Y. K. Min, S. Y. Lee and B. T. Lee, Effect of Local Sustainable Release of BMP2-VEGF from Nano-Cellulose Loaded in Sponge Biphasic Calcium Phosphate on Bone Regeneration, *Tissue Eng., Part A*, 2015, **21**(11–12), 1822–1836, DOI: 10.1089/ten.tea.2014.0497.

135 M. Ramazanoglu, *et al.*, Bone response to biomimetic implants delivering BMP-2 and VEGF: An immunohistochemical study, *J. Craniomaxillofac. Surg.*, 2013, **41**(8), 826–835, DOI: 10.1016/j.jcms.2013.01.037.

136 C. Schlickewei, *et al.*, A bioactive nano-calcium phosphate paste for in-situ transfection of BMP-7 and VEGF-A in a rabbit critical-size bone defect: results of an *in vivo* study, *J. Mater. Sci.: Mater. Med.*, 2019, **30**, 2, DOI: 10.1007/s10856-019-6217-y.

137 N. W. Marion and J. J. Mao, Mesenchymal Stem Cells and Tissue Engineering, *Methods Enzymol.*, 2006, **420**, 339–361, DOI: 10.1016/S0076-6879(06)20016-8.

138 W. Supphaprasitt, *et al.*, A Three-Dimensional Printed Polycaprolactone–Biphasic-Calcium-Phosphate Scaffold Combined with Adipose-Derived Stem Cells Cultured in Xenogeneic Serum-Free Media for the Treatment of Bone Defects, *J. Funct. Biomater.*, 2022, **13**(3), 93, DOI: 10.3390/jfb13030093.

139 M. Brennan, *et al.*, Biomimetic versus sintered macroporous calcium phosphate scaffolds enhanced bone regeneration and human mesenchymal stromal cell engraftment in calvarial defects, *Acta Biomater.*, 2021, **135**, 689–704, DOI: 10.1016/j.actbio.2021.09.007.

140 M. H. Mankani, S. A. Kuznetsov and P. G. Robey, Formation of hematopoietic territories and bone by transplanted human bone marrow stromal cells requires a critical cell density, *Exp. Hematol.*, 2007, **35**(6), 995–1004, DOI: 10.1016/j.exphem.2007.01.051.

141 E. Trouche, *et al.*, Evaluation of alginate microspheres for mesenchymal stem cell engraftment on solid organ, *Cell Transplant.*, 2010, **19**(12), 1623–1633, DOI: 10.3727/096368910X514297.

142 J. C. Roldán, *et al.*, Bone formation and degradation of a highly porous biphasic calcium phosphate ceramic in presence of BMP-7, VEGF and mesenchymal stem cells in an ectopic mouse model, *J. Craniomaxillofac. Surg.*, 2010, **38**(6), 423–430, DOI: 10.1016/j.jcms.2010.01.003.

143 H. Sun and H. L. Yang, Calcium phosphate scaffolds combined with bone morphogenetic proteins or mesenchymal stem cells in bone tissue engineering, *Chin. Med. J.*, 2015, **128**(8), 1121–1127, DOI: 10.4103/0366-6999.155121, Chinese Medical Association.

144 J. R. Overman, M. N. Helder, C. M. Ten Bruggenkate, E. A. J. M. Schulten, J. Klein-Nulend and A. D. Bakker, Growth factor gene expression profiles of bone morphogenetic protein-2-treated human adipose stem cells seeded on calcium phosphate scaffolds *in vitro*, *Biochimie*, 2013, **95**(12), 2304–2313, DOI: 10.1016/j.biochi.2013.08.034.

145 L. Zhao, M. Tang, M. D. Weir, M. S. Detamore and H. H. K. Xu, Osteogenic media and rhBMP-2-induced differentiation of umbilical cord mesenchymal stem cells encapsulated in alginate microbeads and integrated in an injectable calcium phosphate-chitosan fibrous scaffold, *Tissue Eng., Part A*, 2011, **17**(7–8), 969–979, DOI: 10.1089/ten.tea.2010.0521.

146 T. Kai, G. Shao-Qing and D. Geng-Ting, *In Vivo* Evaluation of Bone Marrow Stromal-Derived Osteoblasts-Porous Calcium Phosphate Ceramic Composites as Bone Graft Substitute for Lumbar Intervertebral Spinal Fusion, *Spine*, 2003, **28**(15), 1653–1658.

147 M. U. Munir, S. Salman, A. Ihsan and T. Elsaman, Synthesis, Characterization, Functionalization and Bio-Applications of Hydroxyapatite Nanomaterials: An Overview, *Int. J. Nanomed.*, 2022, **17**, 1903–1925, DOI: 10.2147/IJN.S360670.

148 D.-E. Radulescu, O. R. Vasile, E. Andronescu and A. Ficai, Latest Research of Doped Hydroxyapatite for Bone Tissue Engineering, *Int. J. Mol. Sci.*, 2023, **24**(17), 13157, DOI: 10.3390/ijms241713157.

149 Y. Jiang, Z. Yuan and J. Huang, Substituted hydroxyapatite: a recent development, *Mater. Technol.*, 2020, **35**(11–12), 785–796, DOI: 10.1080/10667857.2019.1664096.

150 M. Somoza, *et al.*, Microfluidic Fabrication of Gadolinium-Doped Hydroxyapatite for Theragnostic Applications, *Nanomaterials*, 2023, **13**(3), 501, DOI: 10.3390/nano13030501.

151 E. A. Ofudje, A. I. Adeogun, M. A. Idowu and S. O. Kareem, Synthesis and characterization of Zn-Doped hydroxyapatite: scaffold application, antibacterial and bioactivity studies, *Heliyon*, 2019, **5**(5), e01716, DOI: 10.1016/j.heliyon.2019.e01716.

152 G. Chen, *et al.*, A postsynthetic ion exchange method for tunable doping of hydroxyapatite nanocrystals, *RSC Adv.*, 2017, **7**(89), 56537–56542, DOI: 10.1039/C7RA10516A.

153 V. Uskoković, Ion-doped hydroxyapatite: An impasse or the road to follow?, *Ceram. Int.*, 2020, **46**(8), 11443–11465, DOI: 10.1016/j.ceramint.2020.02.001.

154 T. Matsumoto, *et al.*, Hydroxyapatite particles as a controlled release carrier of protein, *Biomaterials*, 2004, **25**(17), 3807–3812, DOI: 10.1016/j.biomaterials.2003.10.081.

155 W. J. King and P. H. Krebsbach, Growth factor delivery: How surface interactions modulate release *in vitro* and *in vivo*, *Adv. Drug Delivery Rev.*, 2012, **64**(12), 1239–1256, DOI: 10.1016/j.addr.2012.03.004.

156 C. Xie, *et al.*, Pulse Electrochemical Driven Rapid Layer-by-Layer Assembly of Polydopamine and Hydroxyapatite Nanofilms *via* Alternative Redox *in Situ* Synthesis for Bone Regeneration, *ACS Biomater. Sci. Eng.*, 2016, **2**(6), 920–928, DOI: 10.1021/acsbiomaterials.6b00015.

157 M. Lind, S. Overgaard, T. Nguyen, B. Ongpipattanakul, C. Bunger and K. Søballe, Transforming growth factor-6 stimulates bone ongrowth: Hydroxyapatite-coated implants studied in dogs, *Acta Orthop. Scand.*, 1996, **67**(6), 611–616, DOI: 10.3109/17453679608997766.

158 É. R. Oliveira, *et al.*, Advances in Growth Factor Delivery for Bone Tissue Engineering, *Int. J. Mol. Sci.*, 2021, **22**(2), 903, DOI: 10.3390/ijms22020903.

159 R. Rohanizadeh and K. Chung, Hydroxyapatite as a Carrier for Bone Morphogenetic Protein, *J. Oral. Implantol.*, 2011, **37**(6), 659–672, DOI: 10.1563/AAID-JOI-D-10-00005.

160 M. Dey and I. T. Ozbolat, 3D bioprinting of cells, tissues and organs, *Sci. Rep.*, 2020, **10**(1), 14023, DOI: 10.1038/s41598-020-70086-y.

161 A. Schwab, R. Levato, M. D'Este, S. Piluso, D. Eglin and J. Malda, Printability and Shape Fidelity of Bioinks in 3D Bioprinting, *Chem. Rev.*, 2020, 11028–11055, DOI: 10.1021/acs.chemrev.0c00084.

162 D. Van hede, *et al.*, 3D-Printed Synthetic Hydroxyapatite Scaffold With In Silico Optimized Macrostructure Enhances Bone Formation *In Vivo*, *Adv. Funct. Mater.*, 2022, **32**(6), 2105002, DOI: 10.1002/adfm.202105002.

163 C. Mota, D. Puppi, F. Chiellini and E. Chiellini, Additive manufacturing techniques for the production of tissue engineering constructs, *J. Tissue Eng. Regener. Med.*, 2015, **9**(3), 174–190, DOI: 10.1002/term.1635.

164 R. E. Saunders and B. Derby, Inkjet printing biomaterials for tissue engineering: bioprinting, *Int. Mater. Rev.*, 2014, **59**(8), 430–448, DOI: 10.1179/1743280414Y.0000000040.

165 D. Serien and K. Sugioka, Laser Printing of Biomaterials, *Handbook of Laser Micro- and Nano-Engineering*, Springer

International Publishing, Cham, 2021, pp.1767–1798, DOI: 10.1007/978-3-030-63647-0_52.

166 J. B. Costa, *et al.*, Indirect printing of hierarchical patient-specific scaffolds for meniscus tissue engineering, *Bio-Des. Manuf.*, 2019, **2**(4), 225–241, DOI: 10.1007/s42242-019-00050-x.

167 M. Mohammadi, *et al.*, Robocasting of Single and Multi-Functional Calcium Phosphate Scaffolds and Its Hybridization with Conventional Techniques: Design, Fabrication and Characterization, *Appl. Sci.*, 2020, **10**(23), 8677, DOI: 10.3390/app10238677.

168 B. Derby, Inkjet printing ceramics: From drops to solid, *J. Eur. Ceram. Soc.*, 2011, **31**(14), 2543–2550, DOI: 10.1016/j.jeurceramsoc.2011.01.016.

169 W. J. Kim, H.-S. Yun and G. H. Kim, An innovative cell-laden α-TCP/collagen scaffold fabricated using a two-step printing process for potential application in regenerating hard tissues, *Sci. Rep.*, 2017, **7**(1), 3181, DOI: 10.1038/s41598-017-03455-9.

170 V. Melčová, *et al.*, FDM 3D Printed Composites for Bone Tissue Engineering Based on Plasticized Poly(3-hydroxybutyrate)/poly(D,L-lactide) Blends, *Polymers*, 2020, **12**(12), 2806, DOI: 10.3390/polym12122806.

171 E. J. Bolívar-Monsalve, *et al.*, Engineering bioactive synthetic polymers for biomedical applications: a review with emphasis on tissue engineering and controlled release, *Mater. Adv.*, 2021, **2**(14), 4447–4478, DOI: 10.1039/D1MA00092F.

172 Y. Kim, *et al.*, Biofabrication of 3D printed hydroxyapatite composite scaffolds for bone regeneration, *Biomed. Mater.*, 2021, **16**(4), 045002, DOI: 10.1088/1748-605X/abcf03.

173 M. Puertas-Bartolomé, A. Mora-Boza and L. García-Fernández, Emerging Biofabrication Techniques: A Review on Natural Polymers for Biomedical Applications, *Polymers*, 2021, **13**(8), 1209, DOI: 10.3390/polym13081209.

174 J. F. Gomes, C. C. Granadeiro, M. A Silva, M. Hoyos, R. Silva and T. Vieira, An Investigation of the Synthesis Parameters of the Reaction of Hydroxyapatite Precipitation in Aqueous Media, *Int. J. Chem. React. Eng.*, 2008, **6**(1), 1–15, DOI: 10.2202/1542-6580.1778.

175 A. Veiga, F. Castro, C. C. Reis, A. Sousa, A. L. Oliveira and F. Rocha, Hydroxyapatite/sericin composites: A simple synthesis route under near-physiological conditions of temperature and pH and preliminary study of the effect of sericin on the biomineralization process, *Mater. Sci. Eng., C*, 2020, **108**, 110400, DOI: 10.1016/j.msec.2019.110400.

176 K. Kandori, T. Kuroda, S. Togashi and E. Katayama, Preparation of Calcium Hydroxyapatite Nanoparticles Using Microreactor and Their Characteristics of Protein Adsorption, *J. Phys. Chem. B*, 2011, **115**(4), 653–659, DOI: 10.1021/jp110441e.

177 A. Domokos, B. Nagy, B. Szilágyi, G. Marosi and Z. K. Nagy, Integrated Continuous Pharmaceutical Technologies—A Review, *Org. Process Res. Dev.*, 2021, **25**(4), 721–739, DOI: 10.1021/acs.oprd.0c00504.

178 A. Gregor, *et al.*, Designing of PLA scaffolds for bone tissue replacement fabricated by ordinary commercial 3D printer, *J. Biol. Eng.*, 2017, **11**(1), 31, DOI: 10.1186/s13036-017-0074-3.

179 J. Russias, *et al.*, Fabrication and *in vitro* characterization of three-dimensional organic/inorganic scaffolds by robocasting, *J. Biomed. Mater. Res., Part A*, 2007, **83A**(2), 434–445, DOI: 10.1002/jbm.a.31237.

180 Y. Yang, *et al.*, Dual-functional 3D-printed composite scaffold for inhibiting bacterial infection and promoting bone regeneration in infected bone defect models, *Acta Biomater.*, 2018, **79**, 265–275, DOI: 10.1016/j.actbio.2018.08.015.

181 C. Shuai, W. Yang, P. Feng, S. Peng and H. Pan, Accelerated degradation of HAP/PLLA bone scaffold by PGA blending facilitates bioactivity and osteoconductivity, *Bioact. Mater.*, 2021, **6**(2), 490–502, DOI: 10.1016/j.bioactmat.2020.09.001.

182 C. Shuai, B. Peng, P. Feng, L. Yu, R. Lai and A. Min, In situ synthesis of hydroxyapatite nanorods on graphene oxide nanosheets and their reinforcement in biopolymer scaffold, *J. Adv. Res.*, 2022, **35**, 13–24, DOI: 10.1016/j.jare.2021.03.009.

183 X. Yang, Y. Wang, Y. Zhou, J. Chen and Q. Wan, The Application of Polycaprolactone in Three-Dimensional Printing Scaffolds for Bone Tissue Engineering, *Polymers*, 2021, **13**(16), 2754, DOI: 10.3390/polym13162754.

184 M. Petretta, *et al.*, Multifunctional 3D-Printed Magnetic Polycaprolactone/Hydroxyapatite Scaffolds for Bone Tissue Engineering, *Polymers*, 2021, **13**(21), 3825, DOI: 10.3390/polym13213825.

185 F. Cestari, M. Petretta, Y. Yang, A. Motta, B. Grigolo and V. M. Sglavo, 3D printing of PCL/nano-hydroxyapatite scaffolds derived from biogenic sources for bone tissue engineering, *Sustainable Mater. Technol.*, 2021, **29**, e00318, DOI: 10.1016/j.susmat.2021.e00318.

186 R. Q. Frazer, R. T. Byron, P. B. Osborne and K. P. West, PMMA: An Essential Material in Medicine and Dentistry, *J. Long-Term Eff. Med. Implants*, 2005, **15**(6), 629–639, DOI: 10.1615/JLongTermEffMedImplants.v15.i6.60.

187 A. Scarano, T. Orsini, F. di Carlo, L. Valbonetti and F. Lorusso, Graphene-Doped Poly(Methyl-Methacrylate) (Pmma) Implants: A Micro-CT and Histomorphometrical Study in Rabbits, *Int. J. Mol. Sci.*, 2021, **22**(3), 1441, DOI: 10.3390/ijms22031441.

188 A. Esmi, Y. Jahani, A. A. Yousefi and M. Zandi, PMMA-CNT-HAp nanocomposites optimized for 3D-printing applications, *Mater. Res. Express*, 2019, **6**, 8, DOI: 10.1088/2053-1591/ab2157.

189 K.-L. Ku, *et al.*, Incorporation of surface-modified hydroxyapatite into poly(methyl methacrylate) to improve biological activity and bone ingrowth, *R. Soc. Open Sci.*, 2019, **6**(5), 182060, DOI: 10.1098/rsos.182060.

190 P. Feng, *et al.*, Characterizations and interfacial reinforcement mechanisms of multicomponent biopolymer based scaffold, *Mater. Sci. Eng., C*, 2019, **100**, 809–825, DOI: 10.1016/j.msec.2019.03.030.

191 P. Feng, *et al.*, Structural and Functional Adaptive Artificial Bone: Materials, Fabrications, and Properties, *Adv. Funct. Mater.*, 2023, **33**(23), 2214726, DOI: 10.1002/adfm.202214726.

192 P. Feng, *et al.*, In Situ Generation of Hydroxyapatite on Biopolymer Particles for Fabrication of Bone Scaffolds

Owning Bioactivity, *ACS Appl. Mater. Interfaces*, 2020, **12**(41), 46743–46755, DOI: 10.1021/acsami.0c13768.

193 J. Anita Lett, *et al.*, Recent advances in natural polymer-based hydroxyapatite scaffolds: Properties and applications, *Eur. Polym. J.*, 2021, **148**, 110360, DOI: 10.1016/j.eurpolymj.2021.110360.

194 S. Mallakpour, E. Azadi and C. M. Hussain, State-of-the-art of 3D printing technology of alginate-based hydrogels—An emerging technique for industrial applications, *Adv. Colloid Interface Sci.*, 2021, **293**, 102436, DOI: 10.1016/j.cis.2021.102436.

195 S. Sancilio, *et al.*, Alginate/Hydroxyapatite-Based Nanocomposite Scaffolds for Bone Tissue Engineering Improve Dental Pulp Biomineralization and Differentiation, *Stem Cells Int.*, 2018, 1–13, DOI: 10.1155/2018/9643721.

196 M. Alipour, *et al.*, The osteogenic differentiation of human dental pulp stem cells in alginate-gelatin/Nano-hydroxyapatite microcapsules, *BMC Biotechnol.*, 2021, **21**(1), 6, DOI: 10.1186/s12896-020-00666-3.

197 Q. Wang, *et al.*, 3D-Printed Atsttrin-Incorporated Alginate/Hydroxyapatite Scaffold Promotes Bone Defect Regeneration with TNF/TNFR Signaling Involvement, *Adv. Healthcare Mater.*, 2015, **4**(11), 1701–1708, DOI: 10.1002/adhm.201500211.

198 S. Ghosh, B. Sarkar, R. Mishra, N. Thorat and S. Thongmee, Collagen Based 3D Printed Scaffolds for Tissue Engineering, *Collagen Biomaterials*, IntechOpen, 2022, DOI: 10.5772/intechopen.103914.

199 C. Z. Liu, Z. D. Xia, Z. W. Han, P. A. Hulley, J. T. Triffitt and J. T. Czernuszka, Novel 3D collagen scaffolds fabricated by indirect printing technique for tissue engineering, *J. Biomed. Mater. Res., Part B*, 2008, **85B**(2), 519–528, DOI: 10.1002/jbm.b.30975.

200 K.-F. Lin, *et al.*, Low-Temperature Additive Manufacturing of Biomimic Three-Dimensional Hydroxyapatite/Collagen Scaffolds for Bone Regeneration, *ACS Appl. Mater. Interfaces*, 2016, **8**(11), 6905–6916, DOI: 10.1021/acsami.6b00815.

201 M. Nikkhah, M. Akbari, A. Paul, A. Memic, A. Dolatshahi-Pirouz and A. Khademhosseini, Gelatin-Based Biomaterials For Tissue Engineering And Stem Cell Bioengineering, *Biomaterials from Nature for Advanced Devices and Therapies*, John Wiley & Sons, Inc., Hoboken, New Jersey, 2016, pp.37–62, DOI: 10.1002/9781119126218.ch3.

202 J. Huang, *et al.*, 3D printed gelatin/hydroxyapatite scaffolds for stem cell chondrogenic differentiation and articular cartilage repair, *Biomater. Sci.*, 2021, **9**(7), 2620–2630, DOI: 10.1039/D0BM02103B.

203 A. Kara, *et al.*, 3D printed gelatin/decellularized bone composite scaffolds for bone tissue engineering: Fabrication, characterization and cytocompatibility study, *Mater. Today Bio*, 2022, **15**, 100309, DOI: 10.1016/j.mtbio.2022.100309.

204 G. H. Nancollas and M. S. Mohan, The growth of hydroxyapatite crystals, *Arch. Oral Biol.*, 1970, **15**(8), 731–745, DOI: 10.1016/0003-9969(70)90037-3.

205 R. Liu, L. Ma, H. Liu, B. Xu, C. Feng and R. He, Effects of pore size on the mechanical and biological properties of stereolithographic 3D printed HAp bioceramic scaffold, *Ceram. Int.*, 2021, **47**(20), 28924–28931, DOI: 10.1016/j.ceramint.2021.07.053.

206 A. Alahnoori, M. Badrossamay and E. Foroozmehr, Characterization of hydroxyapatite powders and selective laser sintering of its composite with polyamide, *Mater. Chem. Phys.*, 2023, **296**, 127316, DOI: 10.1016/j.matchemphys.2023.127316.

207 M. Maas, U. Hess and K. Rezwan, The contribution of rheology for designing hydroxyapatite biomaterials, *Curr. Opin. Colloid Interface Sci.*, 2014, **19**(6), 585–593, DOI: 10.1016/j.cocis.2014.09.002.

208 P. C. Cruz, C. R. Silva, F. A. Rocha and A. M. Ferreira, Mixing Performance of Planar Oscillatory Flow Reactors with Liquid Solutions and Solid Suspensions, *Ind. Eng. Chem. Res.*, 2021, **60**(6), 2663–2676, DOI: 10.1021/acs.iecr.0c04991.

209 A. Veiga, R. Magalhães, F. Castro and A. L. Oliveira, Fabrication of highly tuned calcium phosphate/silk sericin composites: exploring new pathways on skin regeneration, in Annual Conference of the European Society for Biomaterials 2021, [Online]. Available: https://eventclass.org/contxt_esb2021/scientific/online-program/session?s=PS2#s138.

210 Q. Wei, *et al.*, Study the bonding mechanism of binders on hydroxyapatite surface and mechanical properties for 3DP fabrication bone scaffolds, *J. Mech. Behav. Biomed. Mater.*, 2016, **57**, 190–200, DOI: 10.1016/j.jmbbm.2015.12.007.

211 D. F. Fitriyana, *et al.*, The effect of hydroxyapatite concentration on the mechanical properties and degradation rate of biocomposite for biomedical applications, *IOP Conf. Ser.: Earth Environ. Sci.*, 2022, **969**(1), 012045, DOI: 10.1088/1755-1315/969/1/012045.

212 J. Huang, *et al.*, *In vitro* assessment of the biological response to nano-sized hydroxyapatite, *J. Mater. Sci.: Mater. Med.*, 2004, **15**(4), 441–445, DOI: 10.1023/B:JMSM.0000021117.67205.cf.

213 M. Milazzo, *et al.*, 3D Printability of Silk/Hydroxyapatite Composites for Microprosthetic Applications, *ACS Biomater. Sci. Eng.*, 2023, **9**(3), 1285–1295, DOI: 10.1021/acsbiomaterials.2c01357.